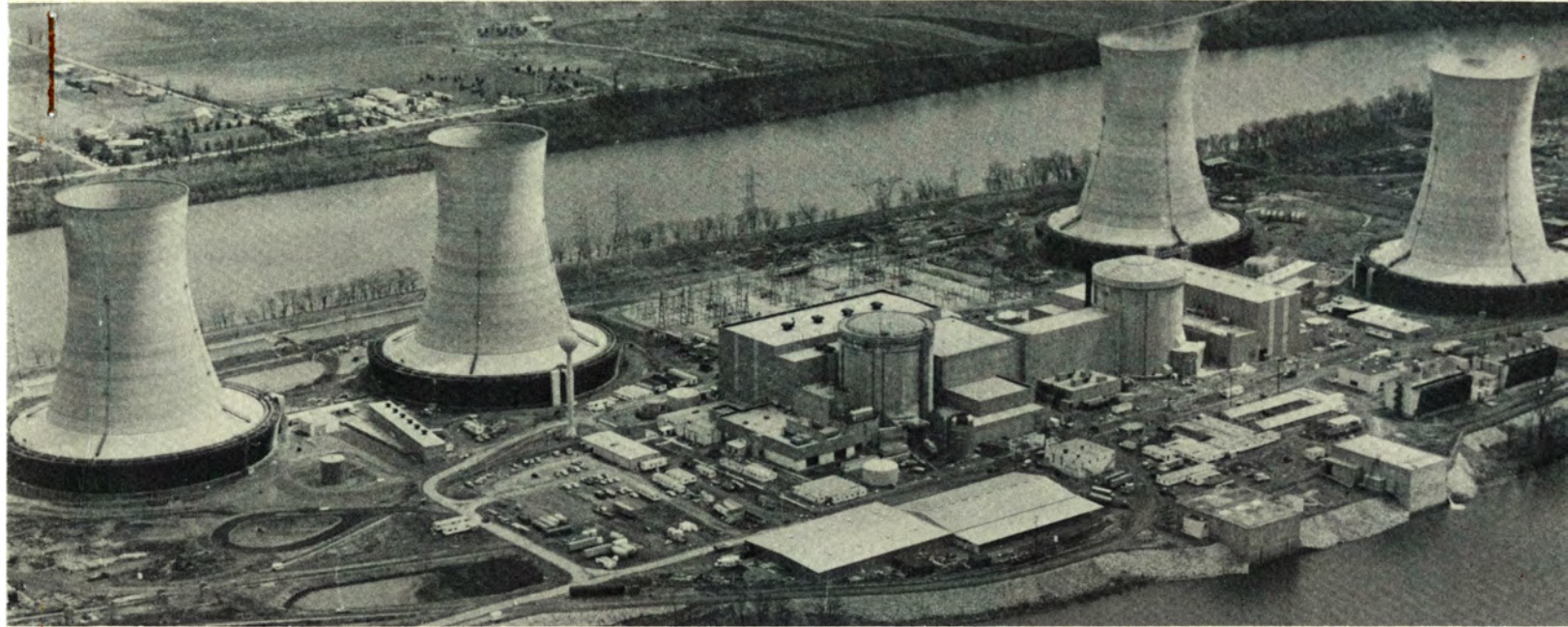


R0083

GEND-INF-012
May 1984



This is an informal report intended for use as a preliminary or working document

GEND

General Public Utilities • Electric Power Research Institute • U.S. Nuclear Regulatory Commission • U.S. Department of Energy

DESIGN AND OPERATION OF THE CORE TOPOGRAPHY DATA ACQUISITION SYSTEM FOR TMI-2

Larry S. Beller
Harry L. Brown

Prepared for the
U.S. Department of Energy
Three Mile Island Operations Office
Under DOE Contract No. DE-AC07-76ID01570

Engin.
TK1345
.H37
T34
1980
R0083



DISCLAIMER

This book was prepared as an account of work sponsored by an agency of the United States Government. Neither the United States Government nor any agency thereof, nor any of their employees, makes any warranty, express or implied, or assumes any legal liability or responsibility for the accuracy, completeness, or usefulness of any information, apparatus, product or process disclosed, or represents that its use would not infringe privately owned rights. References herein to any specific commercial product, process, or service by trade name, trademark, manufacturer, or otherwise, does not necessarily constitute or imply its endorsement, recommendation, or favoring by the United States Government or any agency thereof. The views and opinions of authors expressed herein do not necessarily state or reflect those of the United States Government or any agency thereof.

DESIGN AND OPERATION OF THE CORE TOPOGRAPHY
DATA ACQUISITION SYSTEM FOR TMI-2

Larry S. Beller
Harry L. Brown

Published May 1984

EG&G Idaho, Inc.
Idaho Falls, Idaho 83415

Prepared for the
U.S. Department of Energy
Three Mile Island Operations Office
Under DOE Contract No. DE-AC07-76ID01570

ABSTRACT

Development of effective procedures for recovery from the 1979 accident at the Three Mile Island 2 nuclear station requires a detailed and quantitative description of the postaccident configuration of the core. This report describes the techniques, equipment, and procedures used for making precise ultrasonic, sonar-like measurements of the cavity left in the upper core region as a result of the accident and details the primary results of the measurements.

The system developed for the measurements uses computer techniques for the command and control of remote mechanical and electronic equipment, and for data acquisition and reduction. The system was designed, fabricated, and tested; procedures developed; and personnel trained in 4-1/2 months. The primary results are detailed topographic maps of the cavity. A variety of visual aids was developed to supplement the maps and aid in interpreting companion videotape surveys.

The measurements reveal a cavity of 9.3 m^3 , approximately 26% of the total core volume. The cavity occupies most of the full diameter of the core to an average depth of about 1.5 m and approaches 2 m in places. No more than two of the core's 177 fuel assemblies appear to be totally intact, and only 42 fuel assemblies have any full-length fuel rods remaining. Considerable debris are suspended from the upper grid plate and lines the walls of the cavity. Debris also litter the rubble-strewn floor of the cavity. The results of these measurements include enough detail to assist greatly in clarifying the accident sequence within the core.

ACKNOWLEDGMENTS

Talent and skill from a wide variety of engineering, scientific, and other disciplines, employed with cooperation and enthusiasm, were necessary for the successful completion of the core topography data acquisition project in such a remarkably short time. These people are among those who made important professional contributions to the success of the project, and their work is gratefully acknowledged:

M. R. Martin (Project Manager), B. B. Kaiser (Project Engineer), J. M. Bower, J. L. Clapp, B. E. Empey, D. S. Fee, H. R. Hendricks, J. A. Holm, E. I. Ingram, F. C. Jones, V. D. Klingler, J. Longhurst, W. R. Machacek, K. G. Magill, R. D. Meininger, K. D. Metcalf, C. R. Mikesell, H. G. Miller, Jr., J. D. Mudlin, D. E. Owen, J. R. Pattee, N. K. Rogers, A. M. Rohm, J. W. Rhudy, G. D. Seifert, J. A. Seydel, S. C. Taylor, D. M. Tow, M. E. Whitaker.

In addition, the cooperation and participation of a large number of GPU Nuclear Corporation personnel in operations at TMI-2 are also gratefully acknowledged.

CONTENTS

ABSTRACT	ii
ACKNOWLEDGMENTS	iii
INTRODUCTION	1
PROJECT AND SYSTEM DESCRIPTION	3
Probe and Mechanical System	3
Data Acquisition System	4
Data Processing System	4
SYSTEM DESIGN	7
Transducer Selection	7
Probe System Design	11
Probe	11
Mechanical System	16
Instrumentation and Control	18
Signal Conditioning	22
Timing and Synchronization	25
Motor and Mechanism Control	26
Digital Communications	28
Data Processor	29
Packaging	29
Measurement Techniques	31
Measurements of Range	31
Measurements of Vertical Position	33
Measurements of Speed of Sound	34
Core Cavity Survey	36
Spatial Sampling	37
Data Acquisition Software	38
Initialize	39
Measure Speed of Sound	39
Move Vertically	39
Horizontal Scan	39
Display Data	42
Support and Test Functions	42

Reliability, Maintainability, and Availability	42
Reliability	44
Maintainability	45
Availability	45
TESTING AND TRAINING	47
Testing During Fabrication and Assembly	47
System Operation Tests	48
Personnel Training	51
DATA ACQUISITION AT TMI-2	52
DATA REDUCTION AND ANALYSIS	56
Data Sampling and Redistribution	56
Manual Conditioning	57
View Correlation	57
Contour Checks	57
Computer-Aided Drafting	58
Model Building	58
Error Analysis	58
RESULTS AND DISCUSSION	62
Data Summary	63
Project Overview	70
APPENDIX A	A-1

DESIGN AND OPERATION OF THE CORE TOPOGRAPHY
DATA ACQUISITION SYSTEM FOR TMI-2

INTRODUCTION

Development of effective procedures for recovery from the 1979 accident at the Three Mile Island 2 (TMI-2) nuclear station requires a detailed knowledge of the core configuration following the accident. Remote video surveys of limited scope in the summer of 1982 revealed a cavity in the upper core region that seemed to be about 1.5 m deep, extending out to perhaps two-thirds of the core radius. A clearer, more detailed, and quantitative description of the postaccident core configuration was needed to plan defueling procedures.

This work describes the techniques used for precise ultrasonic, sonar-like measurements of the core void and details the primary results.

The overall objective of this effort was to survey the TMI-2 core cavity in sufficient detail that accurate maps of the postaccident configuration could be made. These maps, augmented by video scans, would provide the majority of the information needed both for developing adequate core recovery procedures and for assembling a scenario of the accident sequence in the core and its outcome. The project schedule allotted five months from start of the core topography data acquisition (CTDA) system design through procurement, assembly, and testing, followed by packaging for shipment.

The principal operating constraint was the limited time interval available to perform a survey. Equipment setup, data acquisition, and equipment removal were to be performed in an eight-hour period. Other operating requirements specifically addressed in the design are related to precision of positioning, service in a radiation environment, and high reliability of equipment to be located in the containment building.

The design constraints governing the overall data acquisition system included requirements that the measuring device:

- Pass through a 38-mm opening left by removal of the lead screw in a control-rod drive mechanism (CRDM)
- Use only one coaxial cable for data transmission from the containment building to remotely located instrumentation
- Use existing wiring for any additional control purposes
- Withstand the general containment building environment (radiation, temperature)
- Tolerate radiation fields up to 10^6 R/hr (in-vessel equipment only)
- Operate in water between 15°C and 60°C (in-vessel equipment only)
- Perform at up to 12 m below the service structure
- Provide 40-mm-lateral and 12-mm-range resolution
- Reflect as low as reasonably achievable (ALARA) policies for radiation exposure to personnel in the containment building
- Measure a cavity of unknown size, geometry, and surface characteristics.

PROJECT AND SYSTEM DESCRIPTION

The required products of the CTDA system were (a) topographic maps accurately depicting the contours of the cavity and any structures within it and (b) detailed scale model(s) built from the maps. The basic technique chosen to gather data for the maps was pulse-echo ultrasonics, where the travel time for short pulses of ultrasound is the measure of the distance or range from the ultrasonic transducer to the first cavity surface encountered by the sound beam. The transducers were designed to produce a narrow and well-collimated sound beam, much like that of a searchlight. A scanning mechanism moved an array of these transducers so that, at the completion of a survey, one or more sound beams had been pointed at all portions of the cavity surface visible from the probe and their locations measured.

The large volume of data required to make accurate maps by this method, together with the requirements placed on measurement precision and overall accuracy, dictated the use of computer techniques for control and data acquisition and reduction.

A brief description of the equipment and its operation is presented here for perspective. Subsequent sections of this report provide more detail.

Probe and Mechanical System

The probe was 35 mm in diameter and about 0.7 m long, on the end of a long boom extending from the upper support structure through a control-rod drive mechanism (CRDM) and the upper plenum into the core cavity (see Figure 1). The probe contained 12 transducers which pointed in 6 different directions ranging from straight down, through horizontal, to 45 degrees from the upward direction. Ten of the transducers were arrayed serially along the length of the probe, while two pointed straight down from the lower tip.

A mechanism on the upper support structure rotated the boom and probe about its axis (sweeping the sound beams through a horizontal plane) and moved it in the vertical direction. These movements were performed by stepping motors under computer control. Digital position encoders provided precise measurements of the vertical and horizontal position of the probe at all times.

Because calibration of the system for range measurements depended on the effective speed of sound in the water of the core (and thus on its temperature and concentrations of dissolved solutes and suspended particles, none of which were well known), it was necessary to provide for precise measurement of the speed of sound in situ.

Data Acquisition System

The command, control, data acquisition, and data storage functions were provided by a minicomputer located outside of reactor containment, about 120 m from the probe. Remote interface electronics were located at the working face on the upper support structure. An overall signal-to-noise ratio exceeding 30 dB for the weakest signals of interest was achieved under these conditions.

Data Processing System

A three-step process was used for data reduction and analysis. In the first step, the raw data were read into a mainframe computer which calculated the absolute locations of each of the first-surface echoes; there were about 5×10^5 of these. These locations were then mapped by the computer onto large-scale plots that showed the locations of all such "hits" within narrow slices of the core volume. Complete sets of slices, 51 mm wide, were taken parallel to each of the three standard orthogonal planes and in full-depth angular (pie-shaped) slices, two degrees wide, about the core vertical axis.

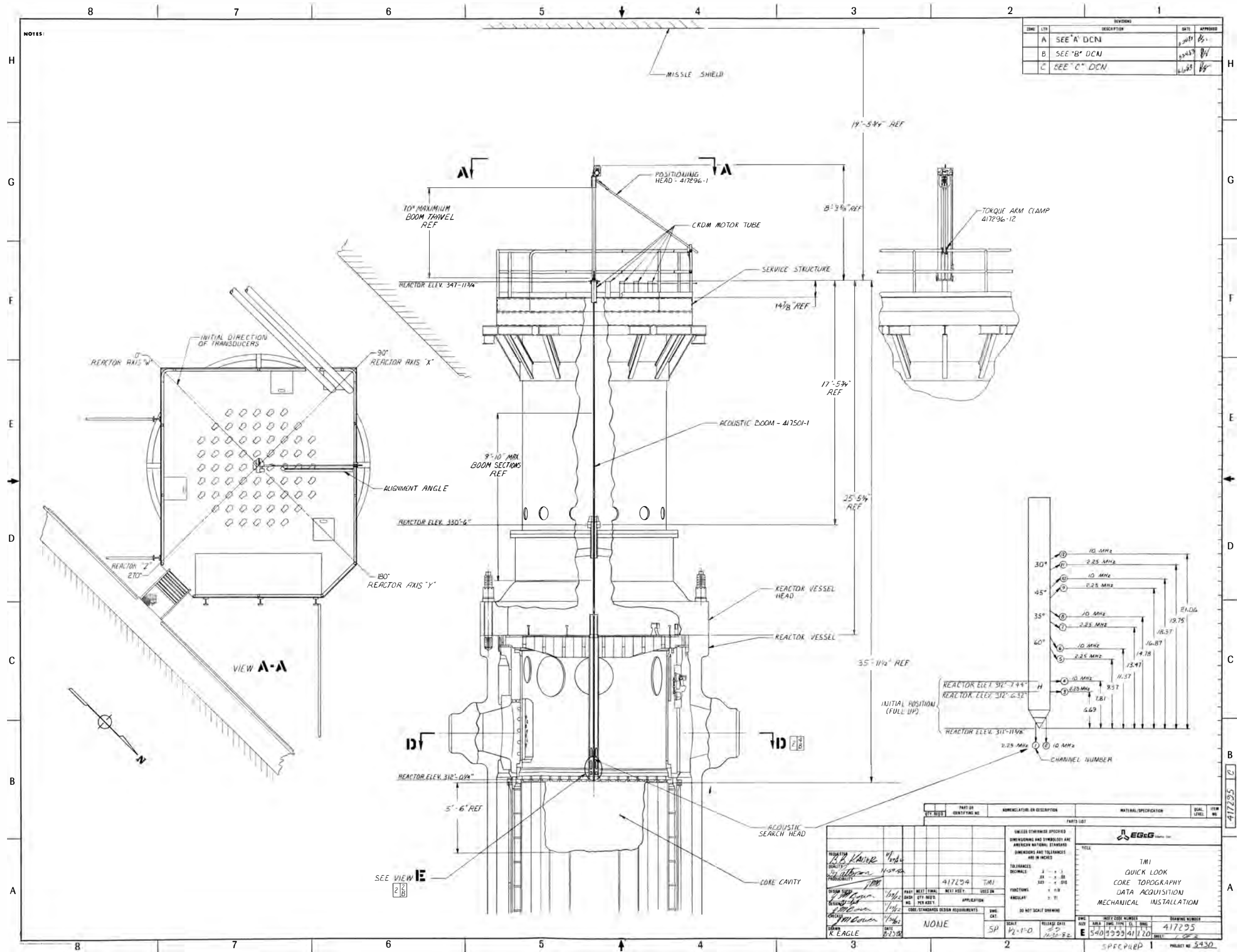


Figure 1. Overall geometry of the upper portion of the reactor vessel, service structure, and core topography data acquisition system access.

Next, data from all four presentations were correlated manually to eliminate most ultrasonic artifacts, to interpolate into and between partially-shadowed areas, and to generate altitude contours (in the horizontal plane). These were entered into a computer-aided drafting (CAD) system by a tablet-entry facility.

Finally, the data were manipulated within the CAD system into a series of topographic maps representing the floor, walls, and top of the cavity. Individual contours were used for making a physical model of the cavity.

SYSTEM DESIGN

Three possible ultrasonic approaches for core topography data acquisition were evaluated from a standpoint of current development status, additional work needed, and overall cost. These were side-looking sonar, synthetic aperture focusing technique, and "searchlight" beam methods. Both the side-looking sonar and the synthetic aperture focusing technique had technical drawbacks or uncertainties with associated risks in further development for this application. Also, overall costs for either were estimated to be higher than that of the multitransducer searchlight beam configuration selected. The following description of the system and component design touches on some of the design constraints.

Transducer Selection

There were two major considerations in selection of transducers for this system. The first was the ultrasonic properties, which depend on frequency; the second was the effective diameter of the sound beam, which determines the resolution of the system.

The attenuation of sound in water is strongly frequency dependent, rising sharply with frequency. Suspended particles could also be expected to affect attenuation. Particle size and concentration were unknown and dependent on the history of prior operations at TMI-2; those particles which would remain suspended for more than a few hours could be expected to have their greatest effect at high frequencies also. These considerations together set an upper limit of roughly 10 MHz on the ultrasonic frequency that could be used reliably. Reflectivity of the surfaces of the cavity is also a complex function of frequency (or wavelength) and of the relative roughness and angle of incidence of the sound beam on the surfaces. In general, one is more likely to obtain a strong reflection at the higher frequencies from rough surfaces, and at lower frequencies from smooth surfaces which are not perpendicular to the direction of sound propagation.

However, the loading of suspended particles, the relative roughness of the surfaces, and the angle of reflective surfaces of the cavity with respect to the direction of the beam could not be known sufficiently well in advance to allow an unambiguous choice of frequency. The solution was a two-frequency system with the two frequencies being sufficiently far apart to cover most of the potential conditions.

The lateral resolution of an ultrasonic mapping system of the type discussed here is simply half of the effective diameter of the sound beam at the point where it strikes a target. Good overall resolution requires that the sound beam have a minimum diameter throughout its usable range. The diameter is determined by diffraction at the transducer aperture and is a function of transducer diameter, d , and the wavelength of sound, λ . The sound beam from a flat-faced transducer can be approximated by the shape shown in Figure 2. There are two principal regions of interest. From the transducer face to what is called the far-field point (FFP), defined by $(d^2 - \lambda^2)/4\lambda$, the beam is nearly parallel, with a diameter about equal to that of the transducer. The beam begins to diverge beyond the FFP. Extensive calculations show that the beam diverges with an initial half-angle that approximates $K \lambda^{1/2}/d$, where K is a constant.

Ideally one would choose a diameter and frequency which place the FFP at the maximum required range. In the present case, this would require either a transducer which is too large to be accommodated in a probe which passes through a 35-mm opening or a frequency which is too high for reliable transmission under the expected conditions. The compromise design for best resolution was a 19-mm diameter transducer having a frequency of 10.0 MHz. The second transducer system was chosen to have the same diameter and a frequency of 2.25 MHz. The beam properties of both are shown in Table 1.

There were two altitude-measuring transducers which pointed straight down. These were 9.5 mm in diameter, at 10.0 and 2.25 MHz respectively, located side by side at the bottom of the probe.

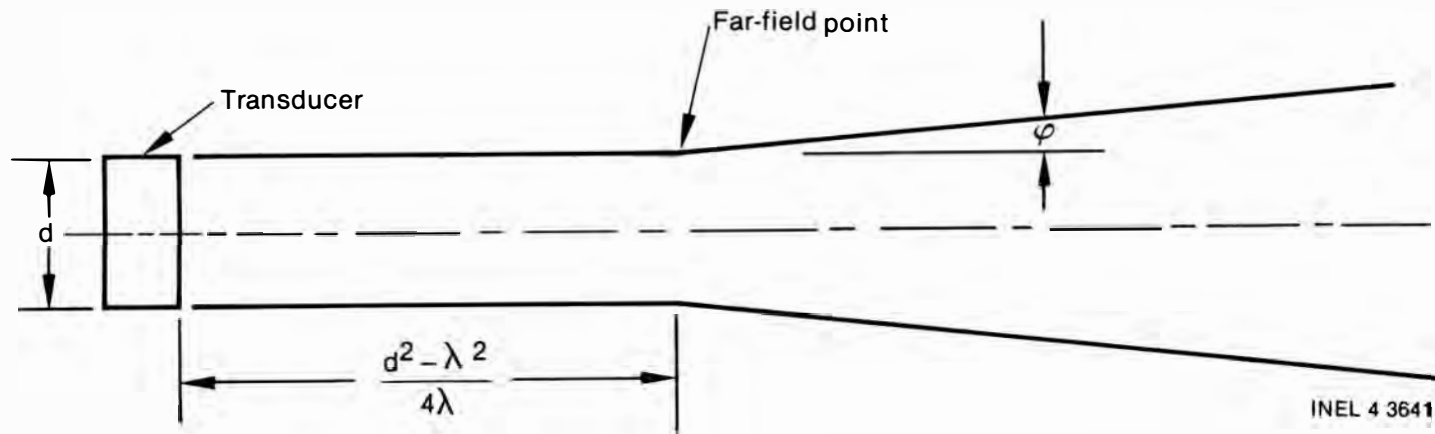


Figure 2. Approximate shape of the sound beam. The cross section of the beam has circular symmetry in a plane perpendicular to the page. The approximate divergence angle for the first few far-field distances is $\kappa \lambda^{1/2}/d$.

TABLE 1. PROPERTIES OF THE ULTRASONIC BEAMS

<u>Transducer Diameter (mm)</u>	<u>Frequency (MHz)</u>	<u>Far-Field Point (mm)</u>	<u>Divergence Half-Angle (Degrees)</u>
19	10.0	600	0.55
19	2.25	140	1.2
9.5 ^a	10.0	150	1.1
9.5 ^a	2.25	34	2.4

a. Transducers for altitude measurement.

Figure 3 is an outline drawing of the probe.

Probe System Design

The overriding considerations for the probe system design were (a) mechanical reliability, (b) adequate sonic coverage of the core cavity, and (c) reproducible and accurate probe positioning for both angular sweep and vertical translation. The principal components of the system were the probe (search head), the probe suspension boom, the horizontal rotation mechanism, the vertical traverse mechanism, and the support structures. The entire system was designed for quick installation and removal to minimize personnel exposure to radiation within the reactor containment building.

Probe

Design of the probe strongly emphasized the need for both adequate sonic coverage and mechanical reliability. The result was an array of transducers (six pairs) fixed in "pockets" milled at appropriate angles in a 75-cm length of stainless steel bar. There were six beam angles: 0, 35, 60, 90, 120, and 135 degrees with respect to the straight-down direction. Two transducers (one of each frequency) were placed side by side for each pointing direction (See Figure 4). The sequence of directions along the probe was chosen for optimum coverage. Scanning coverage is provided by rotating and translating the entire probe assembly.

The polar angles in which the individual transducers were pointed and their sequence along the probe were chosen to provide optimum coverage of cavity surfaces visible from the insertion location, under a series of different assumptions about possible sizes and shapes of the core cavity. For example, the transducer which pointed in the horizontal direction could be expected to produce the most important information under almost any assumptions of cavity size and shape. It was placed at the lower end of the probe, where it emerged first from the plenum (and gathered maximum

information from short cavities) and had the longest possible vertical travel distance under any conditions. The least important transducer was expected to be the 120-degree transducer (30 degrees above the horizontal); it would gather unique information only should the cavity extend to nearly full core radius and be nearly 1.5 m in height. This transducer was placed uppermost on the probe, where it emerged last from the plenum.

The relative coverages of the probe transducers are shown in Figure 5 for an assumed cavity depth of 1.53 m (60 inches) at the location of probe insertion. As can be seen, provision was made to survey "valleys" in the cavity floor in certain locations at least 0.5 m below the level of the probe tip at its insertion point. It will also be noted that there is a "blind" circle centered below the tip of the probe; the circle has a radius of about 0.25 m for a probe height of 0.15 m above the rubble bed. The circle is blind except for the altitude-reading point at its center.

The two altitude-measuring transducers were recessed about 90 mm into cylindrical cavities at the tip of the probe. Machined ledges circumscribed the exit apertures of the cavities to provide small targets intercepting the edges of the sound beams at fixed distances from the transducers. These targets were used to measure the effective speed of sound in the liquid contained between the transducer and ledge. The sides of the cavity were slotted to allow escape of air and exchange of liquid as the probe was lowered.

The necessary R/G-174 coaxial cables (one for each transducer) were fitted into milled slots in the probe bar. The assembly was then backfilled with epoxy resin to protect the cables. The cables were continuous without connectors from the transducer through the probe and boom to the electronics enclosure on the upper support structure to reduce the possibility of trouble associated with water leakage. The probe and boom diameters were 35 mm, permitting passage through the 38-mm diameter opening left by removal of a CRDM lead screw.

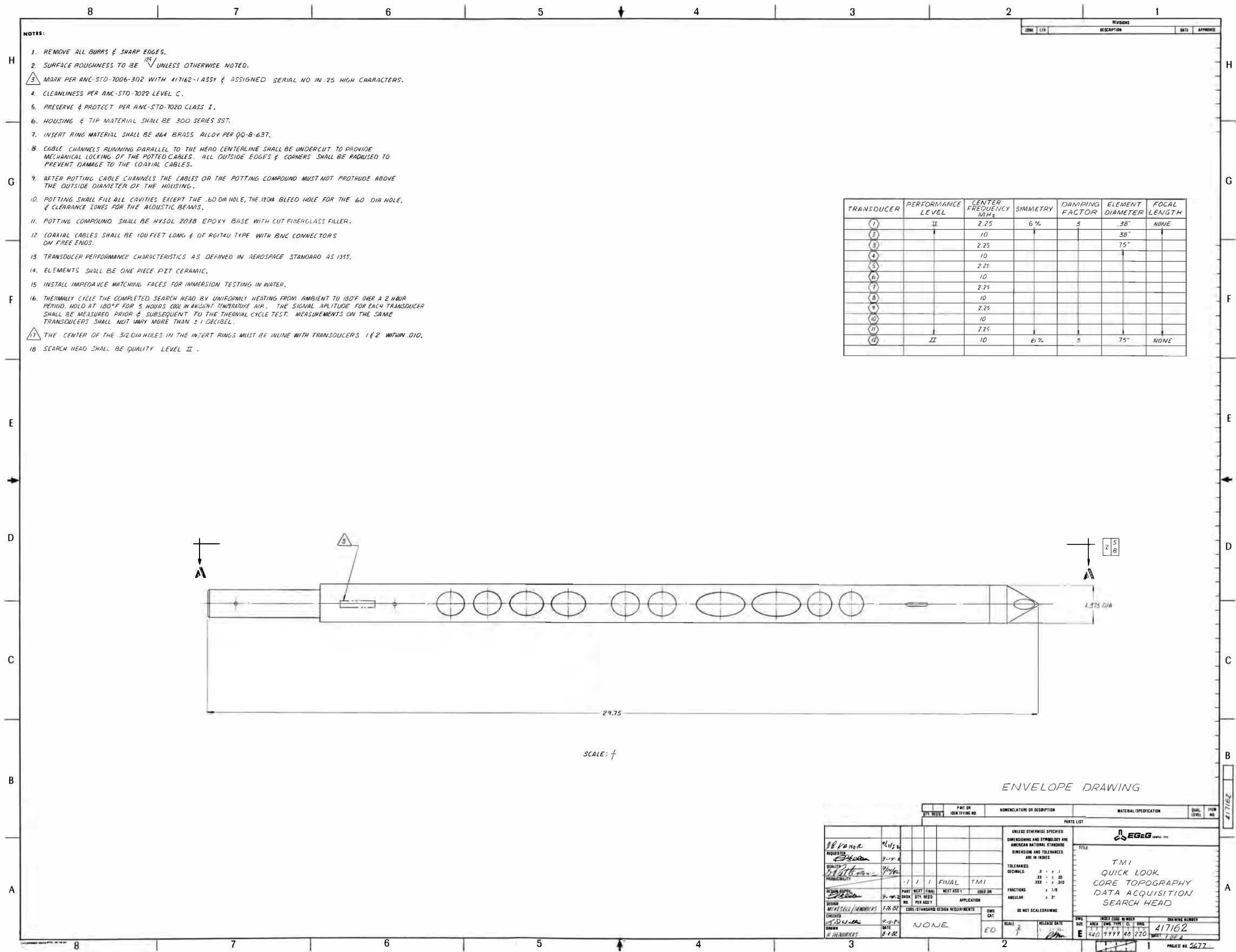


Figure 3. Envelope drawing of the probe. The probe contains 12 transducers. The two altitude-measuring transducers are aligned side by side at the lower tip, which is at the right of the drawing.

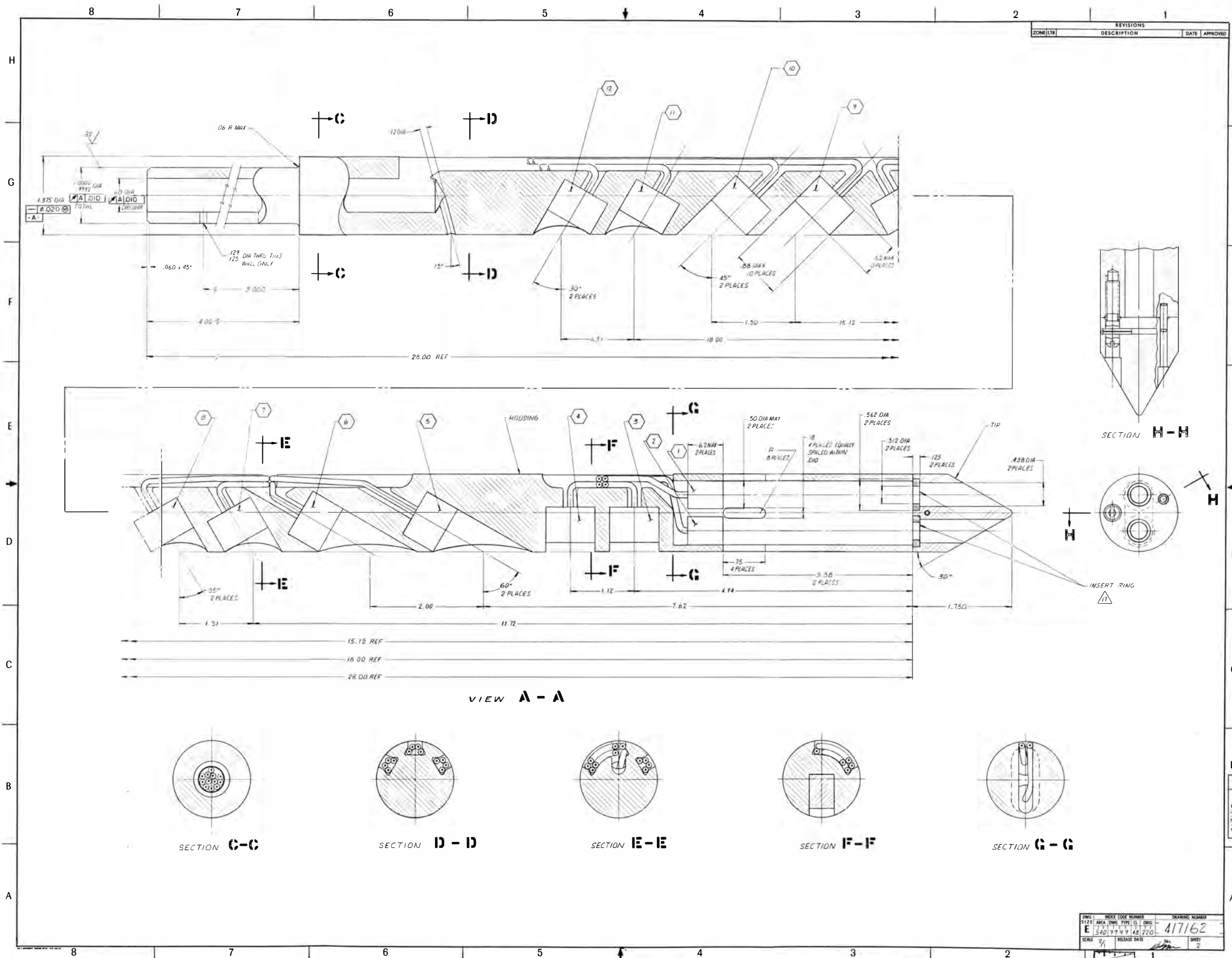


Figure 4. Details of the probe design. The basic probe body was fabricated from a single bar of stainless steel.

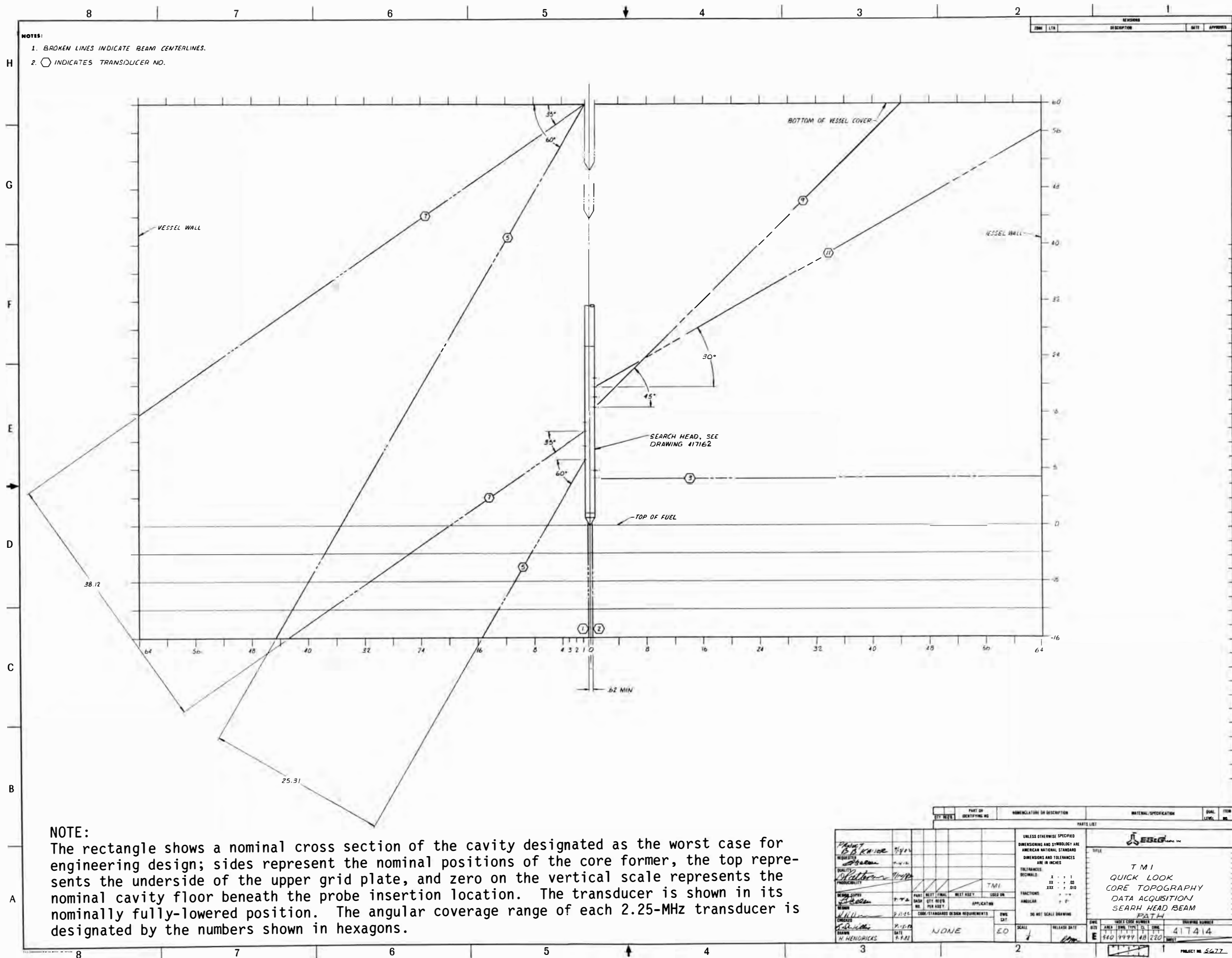


Figure 5. Diagram of ultrasonic ranging coverage for nominal engineering-design cavity size.

Mechanical System

The principal capabilities needed by the system were:

- Horizontal rotation of at least 360 degrees at constant speed
- Vertical translation of 1.8 m in 0.1-mm increments, reproducible up to 12 m below the system base (the CRDM mounting flange)
- Capability for rapid assembly and test in order to comply with the ALARA policy on personnel exposure.

In the assembled system, the probe was attached to a segmented tubular boom extending downward from the drive mechanisms and support structure. The segments were joined to one another and to the probe by screw fittings, pinned at installation. Cables from the 12 transducers were prethreaded through the boom and gathered into a polyethylene sheath for mechanical protection. The boom-and-probe assembly was shipped in its own aluminum container, ready for assembly on top of the reactor (See Figure 6).

The horizontal rotation mechanism, consisting of a 1.8-degree Slo-Syn stepping motor and a right-angle gearbox for rotation, was clamped to the boom with a secure quick-release mechanism. This assembly was suspended from a motor-driven vertical translation device, described below. For horizontal (angular) position readout, a miniature timing belt joined the output shaft to an optical incremental digital encoder. The angular reference was a boom from the horizontal mechanism to the hand railing on the core upper support structure. Angular travel was limited by switches at the 0- and 368-degree locations.

Vertical motion of the probe system and the horizontal traverse mechanism during the core scan was powered by a second 1.8-degree Slo-Syn stepping motor through a right-angle gearbox and a linear chain drive. The lower end of the chain was attached to a spring-loaded takeup reel to

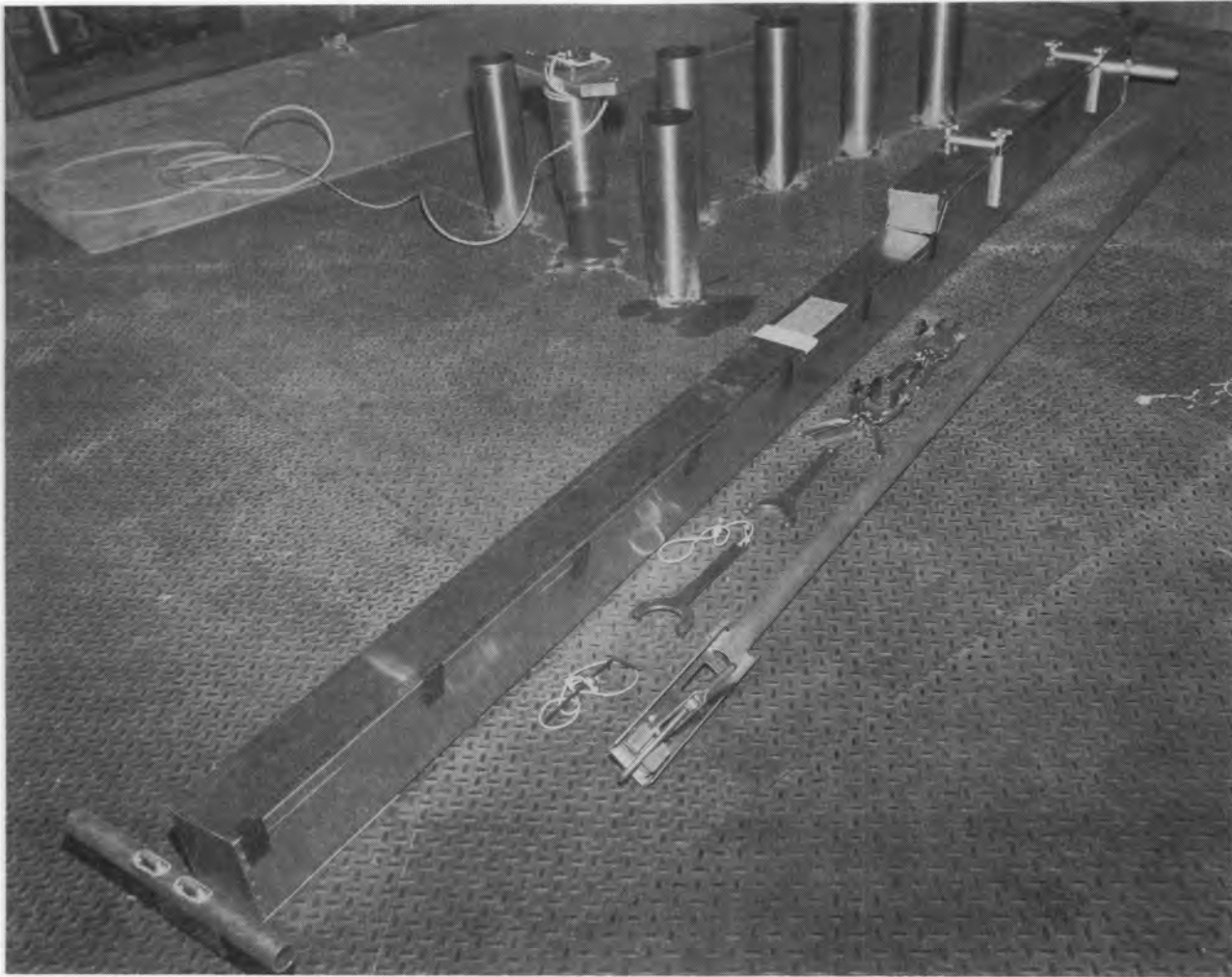


Figure 6. Boom and probe assembly with shipping container. The boom and probe assembly is shown fully assembled to the right of the container. Special tools for assembly and installation are shown between the two. The top of the boom is in the foreground. (EG&G Idaho photo 83-6-1-3.)

assure the necessary tension. Position readout equipment was the same as for angular motion. The mechanisms are shown in Figure 7.

The supporting tower for the system was constructed of two parallel aluminum tubes, which serve as edge guides for the horizontal traverse mechanism. At the upper end, a spacer plate served as a mounting base for the vertical translation motor. At the lower end, a system mounting plate which mated to the available CRDM flange was attached to the tower with cam-action clamps.

Physical assembly began with attachment of the mounting plate to the CRDM flange. The tower, with the vertical drive, was then erected and the horizontal traverse mechanism attached. Next, the probe was attached to the first boom section and inserted through the CRDM opening, leaving enough of one end exposed to permit adding another section conveniently. The exposed portion was double-clamped for safety and rigidity, using specially-modified Vise-Grip clamps. In sequence, the cables were threaded through each subsequent section of the boom, the boom was threaded onto the double-clamped section, the threaded joint pinned, the two boom clamps released sequentially, and the extended boom section with probe again lowered into the core. The operations were repeated until the entire system was assembled.

The completed assembly is shown in Figure 8.

The final step was to test the vertical and horizontal motions quantitatively, as an integral test of mechanisms, circuitry, cabling, and limit devices.

Instrumentation and Control

The instrumentation and control functions are the heart of any ultrasonic measuring system. For the TMI-2 core topography data acquisition effort, the necessary equipment is comprised of electronic gear and a minicomputer. The instrumentation functions were:

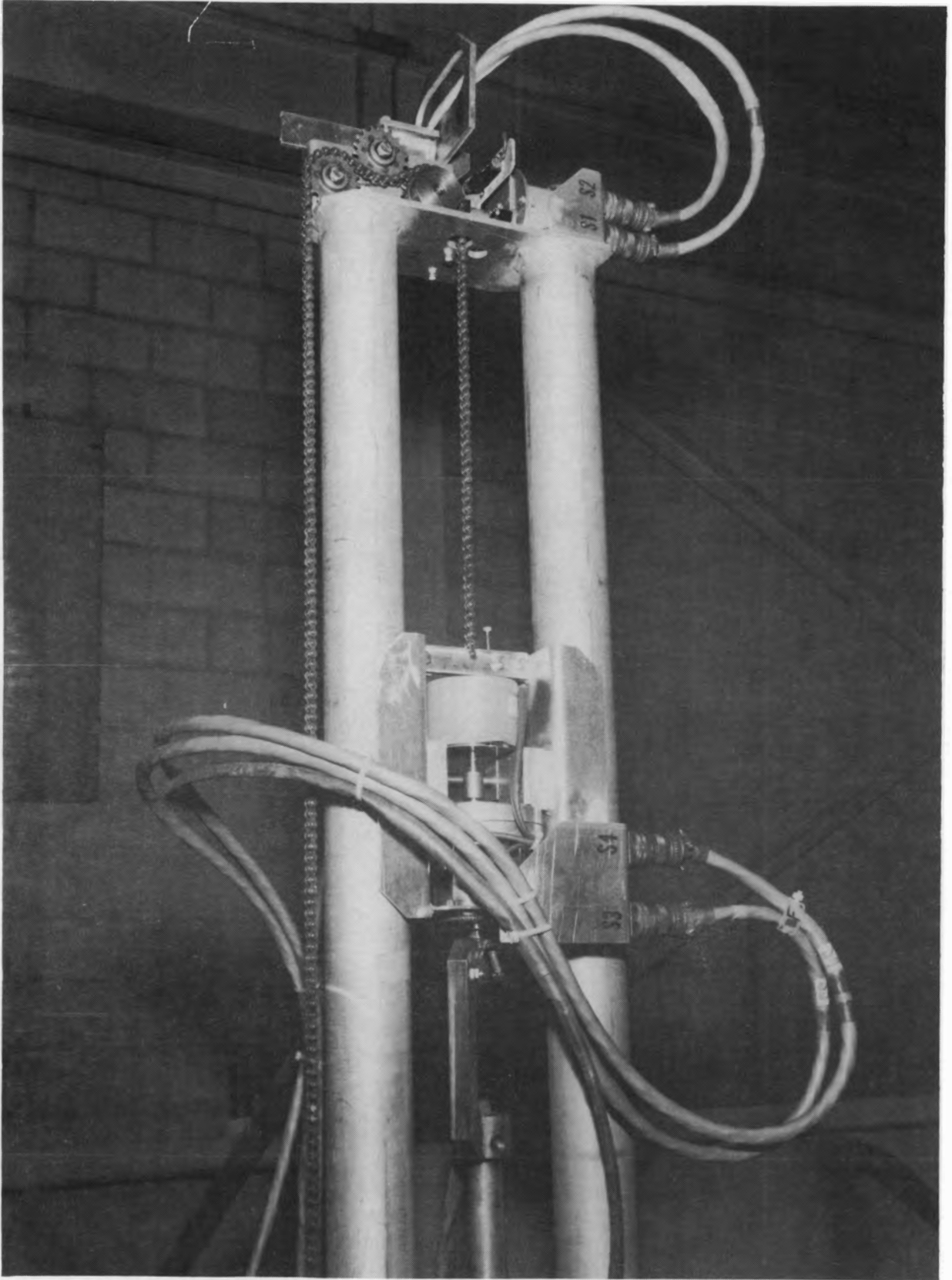


Figure 7. Horizontal and vertical drive mechanisms, installed in the support tower. (EG&G Idaho photo 83-19-1-3.)

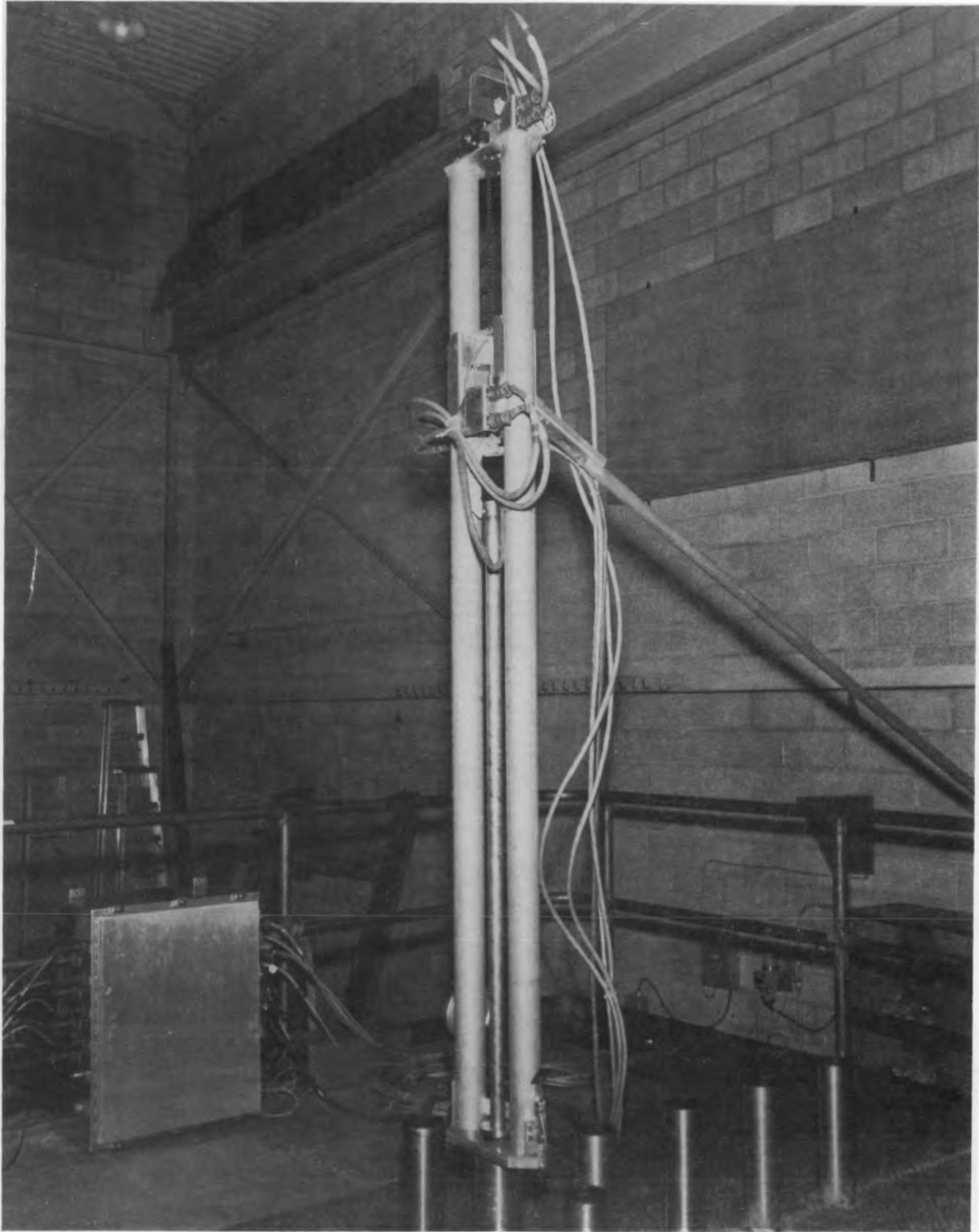


Figure 8. Assembled mechanisms on the mockup service structure.
(EG&G Idaho photo 83-19-1-1.)

- Ultrasonic pulse generation and timing
- Multiplex signal distribution and control
- Return signal conditioning and processing
- Analog-to-digital data conversion
- Data storage and archiving
- Preliminary data processing and display
- Command of all mechanical and electronic test and operation functions, on a selective programmed basis
- Control of all repetitive mechanical and electrical/electronic functions for the ultrasonic scan
- Control of all functions related to data acquisition, processing, storage, and on-line display.

The minicomputer, with its peripherals and supporting electronic devices for data acquisition, handling, and storage, was located outside the reactor containment. Other process and control electronics were installed on the reactor support structure. Data transmittal between the two installations was via a single coaxial cable. Control signals were routed on existing CRDM position readout cabling. The various components and their specified locations are identified in Figure 9. The operational sequence on which the electronic system design was based is described below.

1. Pulses at a clocked repetition frequency are provided by a timing generator. These synchronization pulses are directed to the appropriate pulser-receivers for individual transducers, selected remotely through a multiplexer (MUX).

2. The MUX, operating as a two-level matrix, also directs the receiver output from the returning echo to the signal conditioning system and then to an analog-to-digital converter (ADC). Operation of the ADC is synchronized with the returning signal by means of timing generator pulses which establish an initial delay.
3. Output from the ADC, together with digital position values from horizontal (angular) and vertical position encoders, is then read into the computer memory.
4. The next transducer is selected by the MUX, and the overall sequence is repeated.
5. The data are retained in memory until completion of a horizontal scan, then recorded in a single disk file. The recorded values are read and compared with the original values in memory, bit-by-bit, and any errors encountered are noted.

The recorded ultrasonic data are computer-processed to provide on-line plot displays, speed-of-sound calculations, and probe vertical position information. A description of the actual electronic system is given here in terms of the major functions performed. The applicable categories are (a) signal conditioning, (b) timing and synchronization, (c) motor and mechanism control, (d) digital communication, and (e) data processing. System packaging and its rationale are also included in this description, since it represented an essential portion of the design effort. A block diagram of the system is shown in Figure 10.

Signal Conditioning

Equipment for this function is located both at the working face on the TMI-2 upper support structure (remote) and at the console outside the reactor containment building. Each transducer has its own pulser/receiver. These twelve units are controlled by a two-level MUX (4-bit parallel code, reed-switch operation) which (a) provides direct

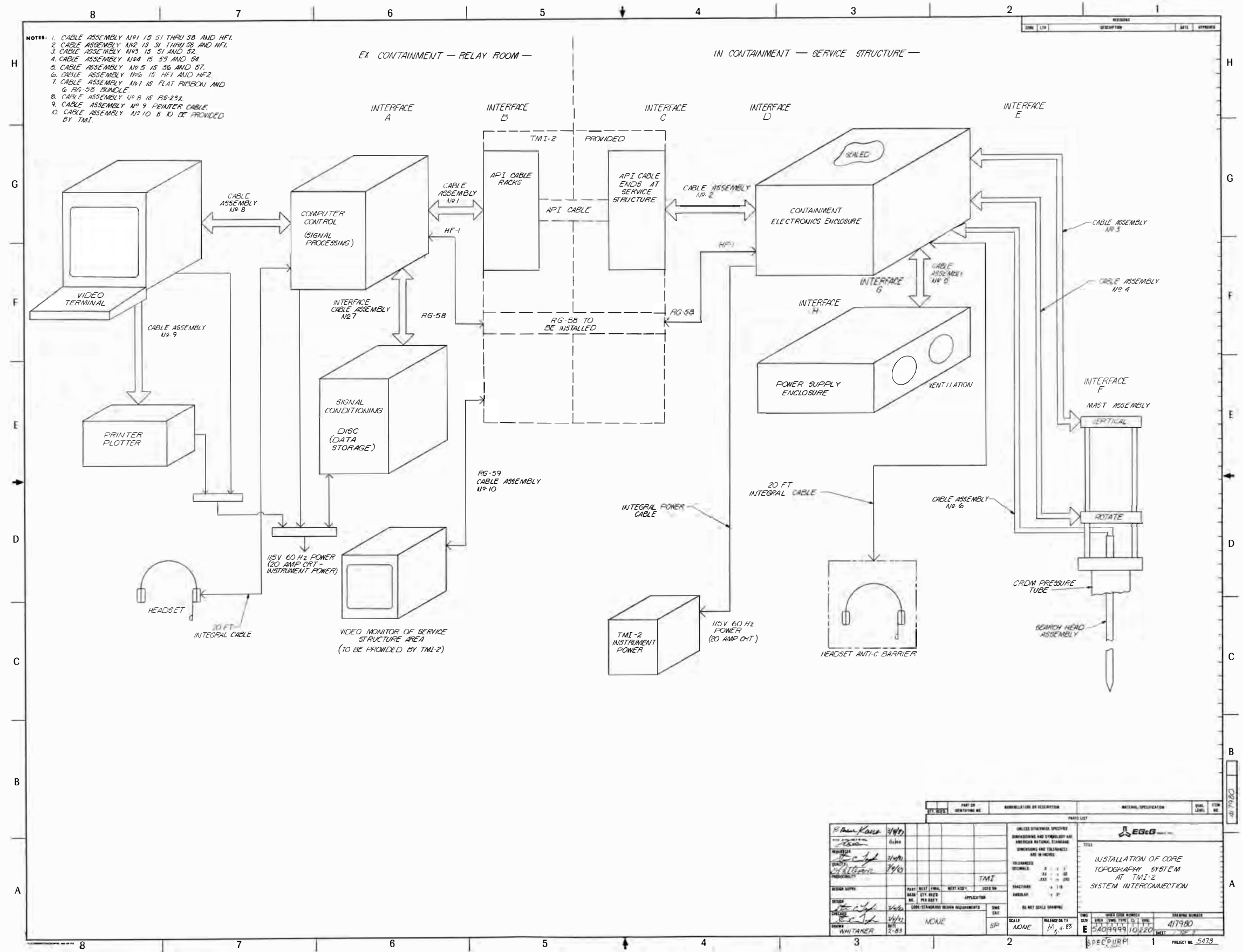


Figure 9. System components, interconnections, and relative locations.

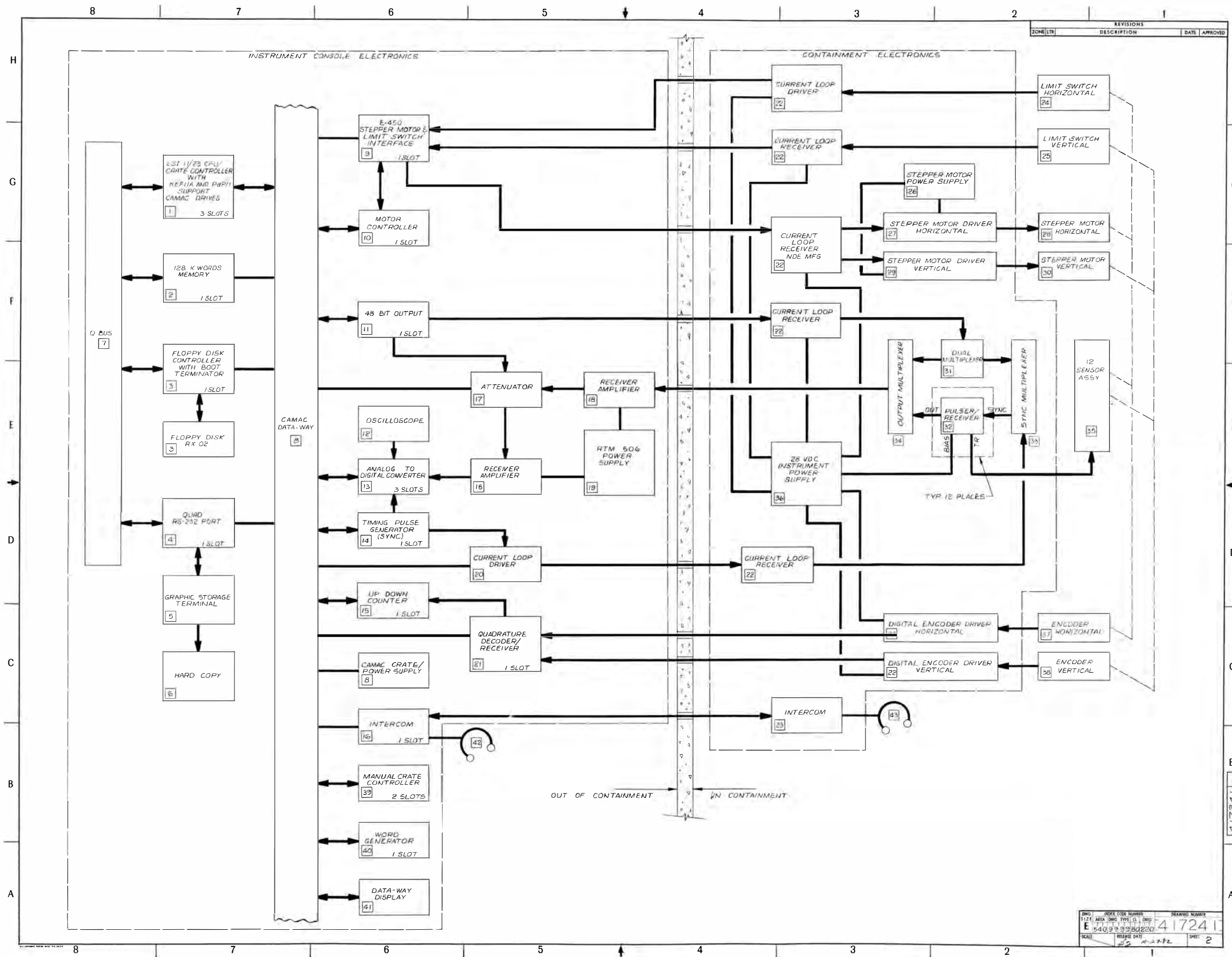


Figure 10. Block diagram of electronic and computer systems.

timing pulse synchronization to the selected pulser and (b) feeds the amplified return signal from the receiver into a 50-ohm coaxial cable to the console. At the console, two receiver-amplifiers provide filtering and manually-selectable gain. These amplifiers are separated by a computer controlled attenuator (64 dB in 0.5 dB steps, reed switch operation) which matches signal gain for each of the selected channels. This step is mandated by differences in range, target reflectivity, and transducer and pulser/receiver characteristics. An 8-bit analog-to-digital flash converter (ADC) processes the conditioned signal, sampling a 30-ps aperture at predetermined intervals of 50 ns to 5 μ s, in a 1, 2, 5 multiplier sequence. The digitized output is accumulated in a 1024-word, on-board buffer memory, which is interrogated by the computer.

Timing and Synchronization

For any ultrasonic ranging scheme, time measurements are converted to distances by means of known propagation velocities. Accurate timing is therefore essential. The two-part timing cycle used here governs physical measurement and data handling for each transducer signal.

The overall timing cycle for each transducer in a sequence involves two nested loops (repetitive timing cycles) which are established by a time-base generator. The length of both loops is set digitally by the software. The inner loop of the time-base generator defines an initial delay from the system synchronization pulse (the time-zero pulse from the generator, which triggers the selected pulser) to the start of the ADC data acquisition cycle. Following the ADC cycle, the software interrogates the contents of the ADC buffer memory, selects the MUX channel corresponding to the next channel in the sequence, and sets the appropriate attenuation for the channel. At the end of the time-base generator's outer loop, typically from 90 to 100 ms, it puts out a new synchronization pulse, and the system recycles with the newly-selected transducer.

The total time, which is the measure of range to target, consists of the time between the synchronization pulse and the ADC memory location

which records the returning echo. The time is then (initial delay) + (ADC memory location number)*(ADC sampling period). Note that the initial delay allows the system to "skip over" areas of no interest near the transducer and distribute the ADC's 1024-word signal sample at fine scale resolution about any particular range region of interest. The length of the outer loop (between transducers) sets the spatial sampling interval at constant probe rotation speed.

A single complete data cycle for one transducer in one location involves the following steps:

- At $t = 0$, pulser is fired; software reads the horizontal position register
- Initial delay established and ADC cycle started
- Data interrogation (software) for establishing pulse propagation and echo time
- Next channel selected
- Attenuation of next channel set
- Initial delay for next channel
- Outer loop timeout completed.

This timing cycle is diagrammed in Figure 11.

Motor and Mechanism Control

Two motor controllers are required for operating the horizontal sweep and the vertical translation stepping motors. Each generates a pulse train, as prescribed by the computer software, which specifies:

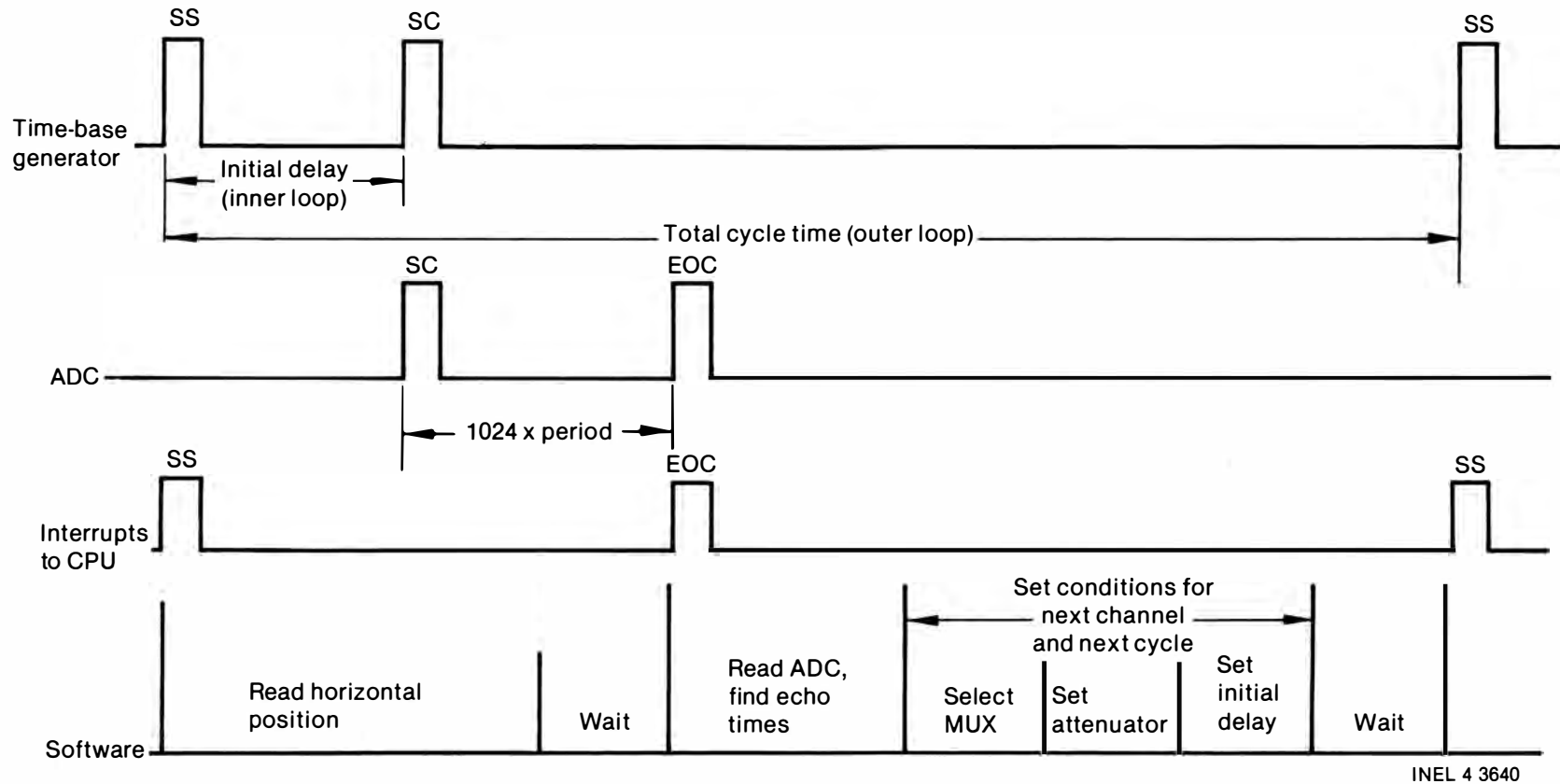


Figure 11. Timing diagram for data acquisition cycle. Abbreviations: SS = system synch ($t = 0$), SC = start conversion, EOC = end of conversion. Approximate times are: total cycle (between SS), 900 ms; initial delay, 40 μ s; ADC cycle, 5 ms.

- Movement direction
- Ramp-up and ramp-down time for the pulse train
- Steady-state pulse rate
- Total number of pulses.

Controller operation stops on actuation of a limit switch in the direction of travel.

Individual motor drivers convert the pulse train to motor drive signals. A stable clock permits extremely close control of the pulse rate and hence the motor rotation speed.

Position readouts for both angular and vertical traverses use two-track, digital-incremental-position encoders mechanically driven by each function. A quadrature decoder senses the position change and direction and provides this information to bidirectional registers. The computer interrogates the register to establish the mechanism's spatial position.

Digital Communications

Design of console-to-containment communication required some care because of high levels of uncontrollable plant-generated electrical noise, with a very real potential for obscuring signals from the data acquisition process. The only available cabling for digital signals consisted of existing straight-wire, CRDM position-readout cabling. Because these were not twisted-pair, they only added to the noise problems.

All digital communications between the console and the containment electronic enclosure were carried on a current-loop system. Input and output were standard TTL signals, but the transmission involved very low-impedance, 20-mA signals between modular senders and receivers.

Experience with these circuits has shown that the very low impedance and the use of current as the variable make it very difficult for noise to induce significant signals on these lines. Such circuits have been used successfully in other applications with up to 500-m cable lengths in very noisy environments. They performed successfully in the present application.

Data Processor

The central processing unit (CPU) was a Digital Equipment Corporation (DEC) LSI-11/23 in Camac format, with an integral Camac crate controller. The CPU included floating point hardware and 256 kilobytes of random-access memory. Mass storage for programs and data was provided by a two-unit, single-sided, dual-density, 8-in. floppy disk system.

The operator's terminal was a Tektronix 4010 storage graphics display with hard copy unit. This combination allowed for both alphanumeric communications and vector graphic output in near-real time with hard copy. An additional raster terminal (DEC VT-102) was used for software development.

Packaging

Design of packaging for the system was influenced by both the operating environment and the need to withstand long-distance shipping. The electronic components at the console, except for the disk systems and the receiver amplifiers, were all in a single Camac crate. Two military-type shipping containers (Figure 12) were used to ensure adequate shock and vibration control. They withstood a rough shipping environment very well.

The remote (in-containment) electronics were packaged in two modules. The containment electronic enclosure was a NEMA Type 12 box which contained the pulser/receivers, multiplexer, motor drives, and digital communications sender/receivers. This unit was sealed against contamination but contained an internal fan to circulate air and improve heat dissipation. The internal dissipation gave the unit a 17°C temperature rise above ambient during operation.

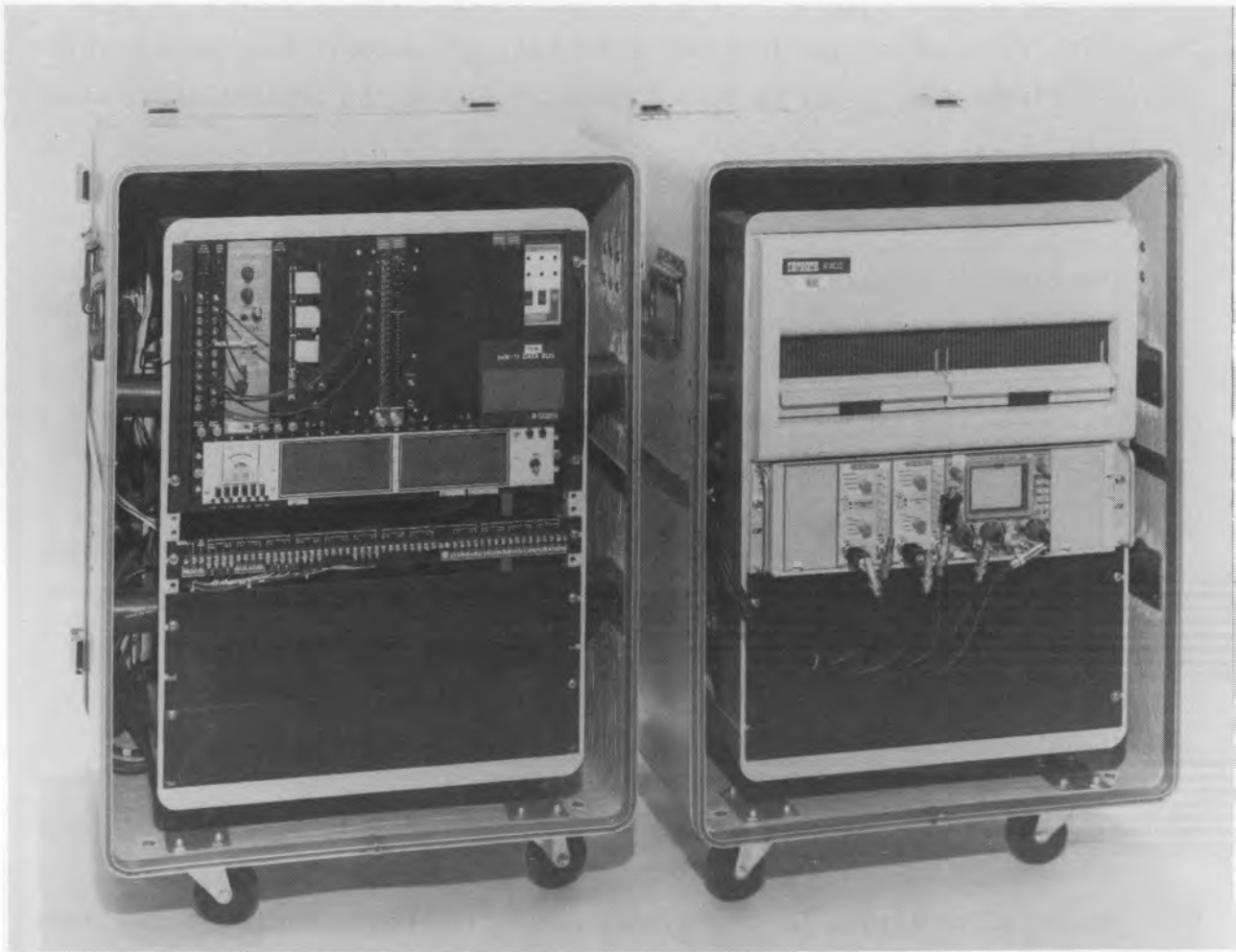


Figure 12. Instrumentation consoles. The Camac crate containing most of the digital electronics is located at the top of the left container. The computer (DEC LSI-11/23) and crate controller occupy the five right-hand slots. The bottom half of the container holds terminal boards and connector strips. At the top of the right-hand container is the disk unit. Below it are the ultrasonic amplifiers and A-scan display. The containers are shock-mounted, military-style units suitable for shipping and use. They are about 0.8 m high. (EG&G Idaho photo 83-62-1-3.)

The motor supply was packaged separately in a fan-cooled and unsealed unit; it was not possible to decontaminate it following use.

The cabling system used captive AN-style connectors throughout. The connectors were numbered, color-coded, and separately keyed for quick assembly and to reduce the possibility of making improper connections. Signal cabling between the enclosure and the probe mechanism was separated physically from motor and encoder cabling and electrostatically shielded.

Measurement Techniques

The hardware and software systems were designed to implement a specific series of methods for surveying the core cavity. These methods are described in this section.

Measurements of Range

Range measurements with the CTDA are defined as those involving measurement of the (slant) distance from a transducer to some target representing the surface of the cavity. Measurements of the altitude of the probe above the floor of the cavity were made in the same way as all other measurements of cavity surface locations. The measured quantity is that of time-to-target echo; it is converted to a measurement of distance through a separately-measured speed of sound, as discussed below.

In each range measurement, time starts with the system synchronization pulse from the time-base generator. After an initial delay which is chosen by the operator, the ADC records the received and amplified echo waveform by sampling it in 1024 equal increments and storing it digitally in a buffer memory. For range measurements, the time of occurrence of the echo is defined as the time when the signal first equals or exceeds a fixed amplitude threshold. Four such thresholds were used. These were set at 20, 40, 60, and 80% of ADC full scale. Immediately following the end of ADC conversion, the software tests the buffer memory and records the memory location (proportional to the time) corresponding to the first crossing of

each threshold. There are thus four separate measurements of range at each point; the separate measurements carry different information which is useful in detecting artifacts and eliminating noise.

To see how this is so, it is necessary to discuss the manner in which amplitude/attenuation (gain) settings are made. Signal amplitude depends on the angle of the reflecting surface with respect to the sound beam, on the roughness of the surface relative to the wavelength of sound, and on the range. None of these quantities could be known in advance of the survey of the cavity, and provision had to be made to accept data over an exceedingly wide range of amplitudes. The system has its highest possible sensitivity for detection of low-amplitude signals when its lowest threshold barely exceeds the noise level of the system; system gain was adjusted to this condition for the first surveys. Since noise has random amplitude, it will occasionally exceed this threshold, however. With reasonably careful adjustment, the same noise spike does not normally exceed higher thresholds.

The principal artifact troubling these measurements is that of multiple reflections. When the surface of the target is uneven, and in particular when it consists of an array of rods, for example, a sound pulse will be subjected to multiple reflections between rods and eventually work its way back to the transducer. It arrives later in time, because of the multiple reflections, than a signal from the first rod encountered in the sequence. Such multiple reflections form "ghost" images behind the first surface. Experiments show that in most such cases the ghost signal is significantly stronger than that from the first rod encountered, presumably because the sound beam strikes the first rod in the series to one side of its center line. Thus, a map of "hit" locations made from data taken at a low threshold will generally show the first surface encountered in this situation, while maps from higher thresholds contain additional surfaces which are ghosts. A comparison of maps made from data at different thresholds will thus reveal the presence of noise and a significant fraction of any multiple reflection artifacts.

At this point it is useful to discuss the way in which system gain adjustments affect effective resolution. The sound beam shapes discussed earlier refer, conventionally, to the half-amplitude points on the side of the sound beam. The sides of the sound beam have a finite slope; they are not vertical, even though they are quite steep. Thus the apparent width of the beam, as measured at a fixed amplitude threshold, depends on signal amplitude and on system gain. If the gain is excessive, a given small target, such as a single rod, will be "smeared" over a wider angular dimension that it would be at a lower gain. At higher gain yet, an isolated target gives the appearance of being bent into an arc centered at the transducer location. This, also, is an undesirable artifact that can be detected by comparison of data from several fixed thresholds. For best results, this particular artifact must be detected and eliminated during an initial reconnaissance survey of the core cavity, before the final survey is made, as discussed below in the section Data Acquisition at TMI-2.

Measurements of Vertical Position

All measurements of vertical location were referred to the position encoder on the vertical traverse mechanism, where the overall accuracy of measurement was of the order of tenths of a millimeter. The zero position on this device was at a limit switch at the upper end of travel. At this location the lower tip of the probe was nominally 16 mm below the lower surface of the upper grid plate.

Altitude measurements refer to range measurements of the distance from the lower tip of the probe to the first reflection obtained from the floor of the cavity directly below the probe. The altitude was measured automatically immediately following each change in vertical position. The measurement was made primarily as a precaution to prevent driving the probe into the floor of the cavity; the measurement was used quantitatively only in locating the elevation of the center of the blind circle directly below the probe.

Measurements of the Speed of Sound

The speed of sound is the basic calibration for the system, and temperature uncertainties presented the largest potential source of error. The temperature coefficient of the speed of sound in water is about 0.15%/°C near 20°C; any errors from this source affect all measurements proportionately. Available information from TMI suggested that the water temperature might vary from less than 20°C to a high approaching perhaps 70°C, depending on the history of recovery operations at TMI in the few weeks or months preceding measurements with this system. The information also suggested that the temperature might vary by five or ten degrees over a period of several hours. There were additional uncertainties concerning the magnitude of effects due to solutes and suspended solids, and convection versus stratification in water temperatures.

It was thus necessary to measure the speed of sound in situ in the cavity and to provide the capability to measure it as a function of vertical position. The measurements were made with the 0-degree (downward-looking) transducers in the geometry discussed above. This geometry provided single targets roughly 90 mm from the faces of the transducer housings.

To make precise measurements in this geometry, it is necessary to know both the effective sound flight path and any time delays between the system synchronization pulse (occurring at $t = 0$, by definition, for the computer and instrument system) and the effective time of emission of the sound wave from the transducer. While the distance from transducer face to target ledge can be measured precisely, it is not clear how to define the flight path from some part of the transducer to the ledge, which is at the very edge of the beam, nor where within the transducer assembly the sound wave is effectively emitted; an epoxy wear face of unknown thickness on the transducer complicates the situation. Time delays of significant magnitude occur in signal propagation through nearly 200 m of cable; in rise times in the digital communications sender/receivers, MUX, and pulser trigger; and in the propagation of the pulser signal across the face of the transducer itself. There are other time delays in the system as well.

The situation can be modeled by

$$c = \frac{x}{t - \epsilon}$$

where t is the observed time of echo return, and x (the effective flight path) and ϵ (the delay time) are constants to be determined by calibration. This is done by measuring t at two different and precisely known speeds of sound, c , then solving simultaneously for the two unknown constants. The speed of sound is changed simply by changing the temperature of pure water; the speed of sound as a function of temperature is well known in the literature. The result is a measurement of the speed of sound which is valid to at least the first order for any liquid within the measurement cavity, and which corrects automatically (again to first order) for thermal expansion of the cavity. Further, if the calibration is done with the same electronic clocks (time-base generator and ADC) that are used during range measurement, systematic inaccuracies in the clocks do not affect the system calibration, provided that the clocks are stable. Second-order errors of small magnitude arise if the temperature coefficient of the contained liquid is radically different from that of pure water.

The time of occurrence of the echo, t , is defined as that of the half-amplitude point on the leading edge of the signal returning from the ledge target. The half-amplitude point so defined yields an elapsed-time measurement which is independent of signal amplitude and of signal rise time. It is measured by recording the signal at 50-ns sampling intervals, finding the signal maximum, and linearly interpolating between the two 50-ns samples that bound the half-amplitude point on the leading edge of the signal. Tests showed that this procedure was accurate and reproducible to less than 3 ns when the signal amplitude was changed by as much as 20 dB. The measurements were made with signal averaging to reduce contributions from system noise.

Calibration was performed at 20°, 30°, and 40°C, and replicated to obtain statistics on precision. Temperatures were measured with a digital

thermometer whose calibration was traceable to the National Bureau of Standards. Statistical analysis of the results indicated a worst-case error of 0.16% over this temperature range, using the derived constants for x and ϵ .

Core Cavity Survey

The design treated data acquisition as a series of independent horizontal scans, in which data were acquired during a full rotation of the probe, preceded automatically by a preselected vertical increment. Each horizontal scan acquired range data from 2000 angular positions which were distributed sequentially among all selected transducer channels; the operator could select from one to five channels to be active on any one horizontal scan, and set the attenuation and initial delay independently for each. Five transducers, covering the full complement of fixed polar angles at a single transducer frequency, was the standard. The operator had the opportunity to change any parameter, including the vertical increment, before beginning a new scan.

The data file for each scan consisted of (a) unique identifying information for the scan, (b) all parameter settings, including those of the ADC, (c) the ultrasonically-measured altitude and vertical encoder reading, and (d) a table of 2000 data sequences consisting of the angular encoder reading and buffer memory locations corresponding to each of the four threshold crossings. At the conclusion of the scan this file was written to the disk, then the disk was read and its contents compared bit-for-bit with memory contents to verify that it had been written correctly. The file for each scan stood alone; it could be retrieved independently under conditions where prior or succeeding files might have been damaged or lost for some reason.

At the conclusion of each scan, the operator had the opportunity to plot the data from any channel during that scan. The plots were in polar form and consisted of range-to-first-surface plotted against angular bearing for a selected threshold. The plots could be scaled arbitrarily at the operator's discretion.

Measurement of the speed of sound could be selected as the next operation following any horizontal scan, at the operator's discretion. The resulting speed of sound was automatically entered into the data file for all succeeding scans until it was measured again. Procedures called for measuring the speed of sound often enough to establish the vertical temperature profile. (The worst case would be temperature stratification; this would cause refraction which would bend the sound beams in a way that would be difficult to correct. Slow convection under stable conditions would cause little difficulty. Convection could be inferred from a higher temperature at the lower elevations. Rate of convection could be inferred from differences in measured speed of sound between successive measurements at a given elevation.)

The lowest permissible altitude was 150 ± 25 mm from the tip of the probe to the floor of the cavity directly below it. This elevation was selected to ensure that the probe was not accidentally driven into the floor of the cavity. Complete surveys started at that point and proceeded upward. Since the boom and probe assembly descended only under the force of gravity, and there remained the possibility that the upper plenum assembly had been distorted during the accident and might interfere with the motion of the boom, upward motion under motor power was considered to present the greatest likelihood of obtaining usable data under adverse conditions.

There were two parts to a survey. The first was a reconnaissance survey of limited scope, designed to establish the principal dimensions and configuration of the cavity, and to optimize transducer selection and operating parameters. The second part was the detailed survey itself.

Spatial Sampling

The volume to be sampled was scanned in 1-in. vertical increments and 368-degree horizontal rotation. The combination of rotational overlap for each scan and sound beam coverage overlap on successive scans ensured that essentially all of the cavity boundary was adequately sampled.

The nominal angular interval for sampling by each transducer is 0.9 degree, i.e., 400 samples per transducer, or slightly greater than one sample per resolution element (defined in terms of the sound beam angle: approximately 1.2 degrees for the 2.25 MHz transducers). Within this interval, five transducers of differing orientation provided time-to-first-echo information for an angular sector of the cavity. The overall sampling rate for the entire cavity, because of redundancy of coverage resulting from the 1-in. vertical increments and overlap of coverage from different polar angles, averages about two per resolution element, an acceptable, but sparse, value.

Data Acquisition Software

The operating system software was Digital Equipment Company (DEC) RT-11, configured for the DEC LSI-11/23 minicomputer. The assembly language (used for the inner data acquisition loop and most of the low-level drivers) was Macro-11. All else was written in FORTRAN.

All operating parameters of the software, including transducer selection, attenuations, initial delays, constants, scaling factors, etc., were located in a default table that was compiled as part of the applications program. Any and all of these values could be modified by the operator at any time.

The main applications program was menu-driven; at the conclusion of any operation the operator was presented with a menu of possible functions from which to choose. Choice of a major operation generally presented the operator with an additional submenu of detailed choices referring to that operation. In each case, one or more of the menu items permitted changing a default-table value.

The main functions of the applications program, with short descriptions of their operation, are given below.

Initialize

This function was generally the first step in starting the system operation. The program drives the two motions of the system continuously in the direction of their zero-position limit switches. On reaching the limit switches, hardware generates an interrupt (telling the program that the motion has reached its limits), and the software clears the position registers, setting them to their zero positions.

Measure Speed of Sound

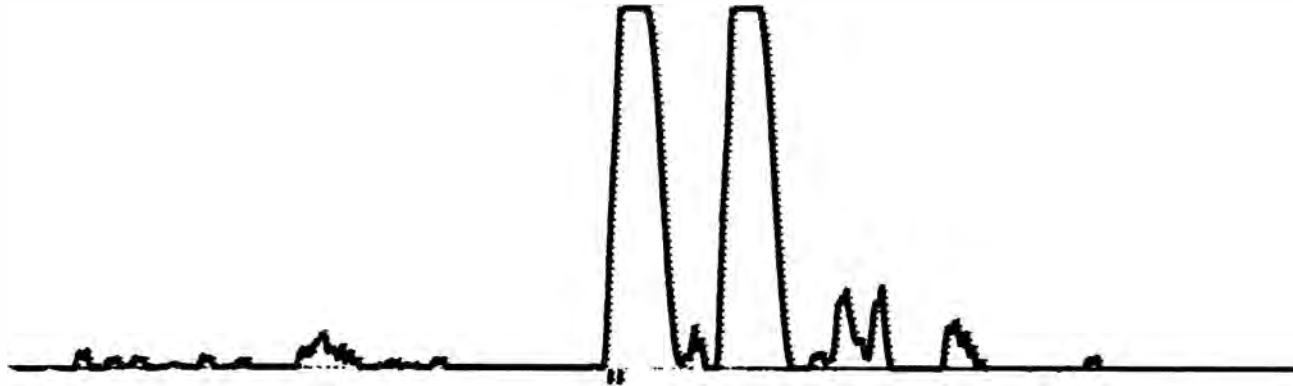
The program executes the routine described earlier for measuring the speed of sound. The routine ends with a display like that shown in Figure 13, giving the waveform obtained from the target (to assure the operator that the operation has been performed properly), the conditions of the measurement, and its results. Procedures called for making at least three such measurements successively each time the routine was used. This gives combined estimates of statistical precision and of possible rate of convection. The last value obtained is entered into the default table automatically.

Move Vertically

The operator may accept the current contents of the default table, or he may specify a new value for direction (+ or -) and the distance to be moved. On completion of the specified movement, the program displays the results of the measurement in the form shown in Figure 14, which again gives the waveform, conditions of measurement, and its result.

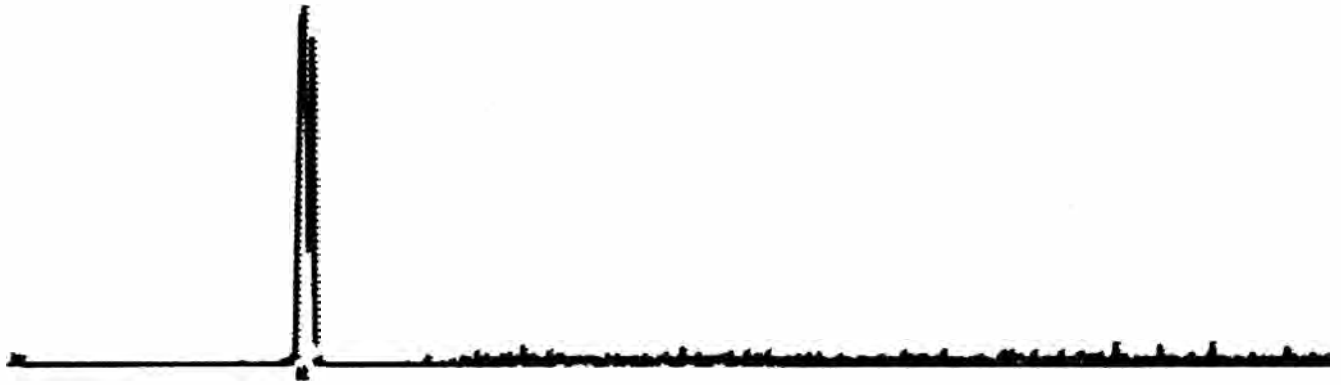
Horizontal Scan

The software performs a horizontal scan, as described above, using the current contents of the default table. The specified vertical movement is first made with a new altitude display as in Figure 14, and the horizontal scan is then made. At the end of the scan the data are recorded on disk and verified.



SPEED SOUND = 59687.88 INCH/SEC TIME TRAVEL = 122.4369
 MAXP = 255.0000 SETPOINT = 127.5000 BIN # 448
 DELAY TIME = 100.0000 CHAN = 2 PERIOD = 5.0600001E-02

Figure 13. Display from sound measurement at TMI-2. This is a display of the signal trace as recorded by the ADC. Time runs from left to right. Times are listed in microseconds. The speed-of-sound target ledge is seen as a pair of large signals. Both edges of the target are visible. The first large signal is used for the measurement. The smaller signals represent minor roughness of the sides of the measurement cavity. The two tick-marks at the baseline below the target signal show the locations of the two ADC "bins" spanning the half-maximum point on the leading edge of the signal.



DIS. TO BOTT = 34.92460 INCH TIME TRAVEL = 1.410000E-03
MAXP = 255.0000 SETPOINT = 127.5000 BIN # 212
DELAY T. 350.0000 CHAN 1 PERIOD = 5.000000

Figure 14. Altitude measurement display. The large spike on the signal trace is the echo from the bottom of the cavity directly below the probe. Delay time (T) and period (ADC) are given in microseconds.

Display Data

This function produces a polar plot of range-and-bearing data discussed above. The operator can select any channel (or all channels successively) and the threshold desired; he may also select an arbitrary scale and define the location of the plot on the screen area. An example from TMI-2 is shown in Figure 15. Plots are normally made with data from the preceding horizontal scan, which is still in memory until a new scan commences; a separate routine was used to specify and plot a file resident on the disk.

The procedures called for plotting the horizontal-transducer data following each scan; this is the only transducer for which the data are easy to interpret in the range-and-bearing form. The procedures called for plotting at least one additional, and different, channel following each scan. This was used to verify channel operation and the adequacy of gain and delay settings on a continuing basis.

Support and Test Functions

This category of software provided a miscellaneous collection of functions which were useful in testing the system and diagnosing faults. Among these functions were:

- (a) Test transducer. Select a specified transducer and fire it repetitively.
- (b) Initialize and verify disk. This function wrote the timing information on a new disk and verified that its entire area could be used. Procedures called for removing and destroying any disk that had any bad areas.

Reliability, Maintainability, and Availability

The overall objective of system design in all its hardware, software, procedural, and personnel aspects was to ensure as nearly as possible the

FILE N.DY1:F18.TMI

CHANNEL 3
SET POINT 100
SCALE F. 6.
SPEED S. 59674.
DATE 8/31/83
TIME 13:36
FROM TOP 36.1
FROM BOTTOM 21.6

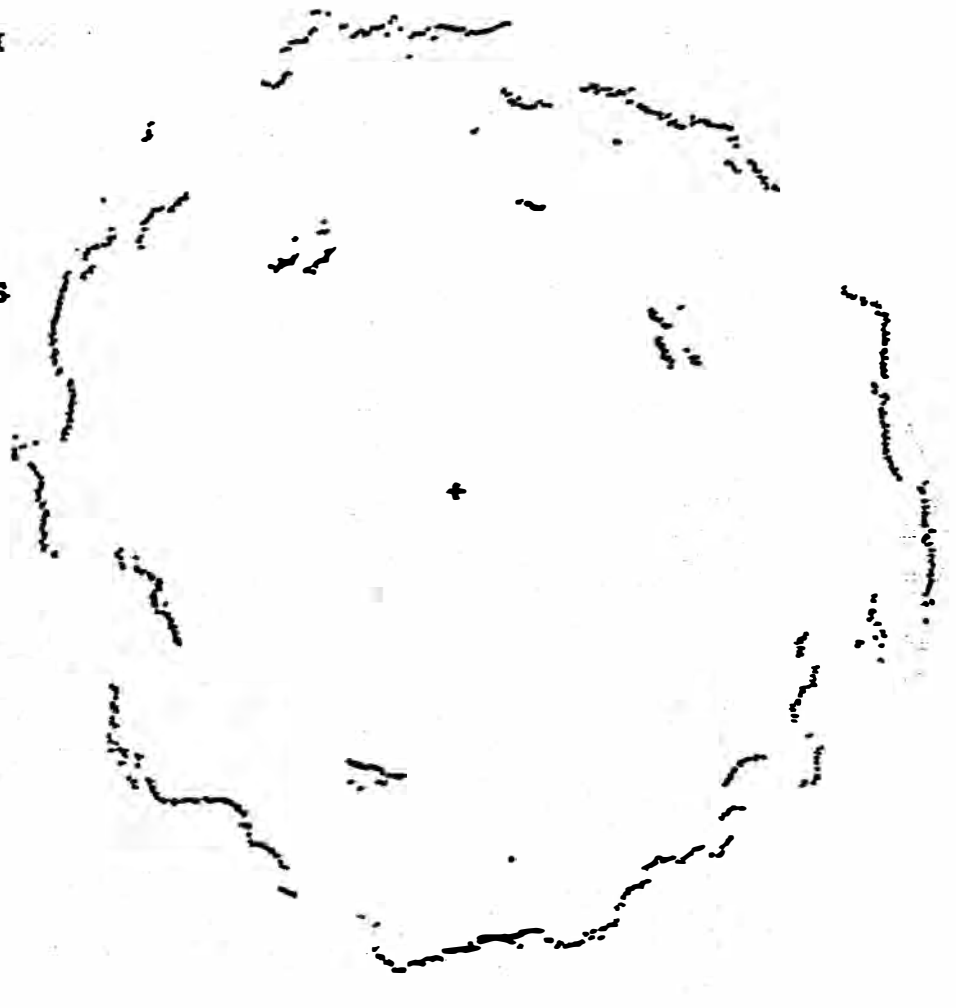


Figure 15. Typical on-line range-and-bearing plot from TMI-2. Channel 3 is the 90-degree (horizontally-pointing) transducer. "Set Point 100" refers to the second threshold. Scale factor (F) 6 is an arbitrary scaling factor proportional to the size of the plot on the screen. Speed of sound (S) is given in inches/second. Distances "from top" and "from bottom" are given in inches of travel from the top limit switch and the ultrasonically-measured altitude, respectively. The scale bar at the lower left is 12 inches long, with tick marks each four inches. The cross at the center shows the probe location. Four axial power shaping rods appear at this altitude at locations between the probe and cavity walls; the structure in the west-southwest direction, away from the walls, is seen as an array of fuel rods in Figure 21.

acquisition of sufficient usable data in spite of anything that could go wrong before, during, or after the measurements. "Things that could go wrong" included mechanical or electronic failures, software or procedural bugs, incorrect assumptions about conditions at TMI, human failures, and an accident to or disability of key personnel. The entire program was keyed to ensuring the availability and proper operation of the system during the crucial data acquisition period.

Reliability

Reliability is in large measure a design function, supported by thorough testing at all points. The basic design philosophy was conservatism, using components and methods of proven reliability, extending them as necessary for the application.

With the sole exception of the remote pulser/receivers, the electronic and computer systems were designed to use instruments, modules, and techniques of known high reliability which had been demonstrated in similar use at INEL. The mechanical systems were designed in a similarly straightforward and conservative manner.

The testing program, described in more detail below, was exceptionally thorough. It was designed to test each function, interaction, and interface in detail to ensure conformity to design and freedom from unexpected bugs.

A modified failure modes and effects analysis (FMEA) was performed for each system. The analysis considered each system component down to the module level, its potential failure modes, and for each of these the consequences and remedial actions that would be necessary to continue operation. In a few cases, the FMEA identified weak spots in the designs; these were changed as necessary to increase system reliability. In other cases, the results of the FMEA were used to design fall-back or "fail-soft" methods, usually involving software changes, which would permit continued operation, although at somewhat less efficiency or accuracy if need be,

should a particular difficult to repair component fail. The FMEA also identified the most-needed spares, and helped in formulating a spares and maintenance strategy.

Maintainability

Modularity played the major role in design for rapid and reliable maintenance of the system. The Camac system, which is inherently modular, makes it particularly easy to isolate and repair failures. In a number of cases on-board spares were installed, requiring only quick changes in connections to permit continued operation. In other cases, slide-in replacement modules were available. Fault isolation and diagnosis routines were built into the software and generally available for hardware as well.

A complete set of all manual and schematic diagrams was available during all operations. Documentation included a complete set of interconnection diagrams, including wire lists and signal "road maps," to assist in fault isolation and repair. Maintainability during the crucial data acquisition period was assisted by requiring that the principal system designers be available at TMI.

The major difficulty with maintainability was associated with those components that were located within the reactor containment building. Repair or replacement of these would become very difficult, if not impossible, due to the time required to plan and make an entry and the difficulty of making repairs while wearing the required anticontamination clothing, particularly for the electronic components. The maintainability of the in-containment electronic systems was thus nearly nil. The design relied, instead, on redundancy and fail-soft considerations.

Availability

Appraisal of probable availability of the final system showed a 99% chance of completing a test sequence within an eight-hour interval without failure. For any failure, the estimated time-for-return-to-service was approximately two hours.

In practice, the system exceeded 200 h of full operation during test and use at TMI-2, plus an additional 200 h or more of partial operation during assembly and system integration without failure. This record approaches the estimated mean-time-between-failures, but was not long enough to test it fully.

TESTING AND TRAINING

Throughout this program testing and training were closely integrated. The purposes of both operations were to ensure a properly operating system, operated properly by the personnel. In general, the personnel who designed a system or component were the same ones who fabricated and assembled it, made it work, developed the operating procedures, and were scheduled to operate it at TMI. This rule included procedures and techniques, with the same level as detail as the hardware and software.

Testing During Fabrication and Assembly

All modules had a thorough receiving inspection. This included visual inspection for workmanship, along with detailed functional performance tests in the system which used them in nearly all cases. In addition to checking the performance, this procedure also allowed a thorough test of each interface and developed a knowledge of quirks, idiosyncrasies, and performance limits.

Software paced this process. In view of the short five-month schedule, the software was begun early, before the final computer had been delivered. Software was developed in a series of mainly single-function modules which were available when needed to test the hardware modules as they became available as part of a subsystem. The software was subjected to the standard "desk checks," to functional checks during subassembly and interface assembly and testing, and to overall system tests at the conclusion of assembly. The modular test routines in general became at least the logical framework of the final programs and were available as fault diagnostic routines during system testing and operations.

The probe assembly was subjected to a series of special tests. The manufacturer was required to supply frequency spectra and field pattern measurements obtained both before and after a temperature-cycling test. This test plunged the probe assembly into water at 65°C for a prolonged period, and then allowed it to cool slowly. The test was designed to

simulate worst-case thermal expansion conditions expected at TMI and to ensure the integrity of the potted cable and transducer assemblies under these conditions. Laboratory tests verified the accuracy of the manufacturer's measurements and would have detected shipping damage, had there been any. Laboratory tests were also made with the intention of verifying the specified polar angles for the probe transducers; the acoustic axes of transducers are commonly several degrees offset from the mechanical axes of their cases. The precision of these tests was limited to about one degree by the relatively short water path, less than 0.5 m, available in the laboratory apparatus.

At the conclusion of system assembly and integration, all aspects of the hardware and software systems had been thoroughly tested, and many of the procedures had been at least partially tested. Because of its sheer size (more than 12 m in length, requiring a water path at least 2 m in length to test measurements at full range), the overall system could not be tested directly in a laboratory.

System Operation Tests

The final system tests were performed in a TMI mockup located at the SPERT-II facility at the INEL. The mockup was designed (a) to simulate the environment of the upper service structure at TMI-2 where the system would be assembled and inserted into the reactor and (b) to provide a water-filled chamber of large size, having surfaces and structures which are intended to mock up those which might be encountered within the core cavity at TMI-2.

The mockup service structure was a detailed copy of that at TMI-2, except that only a fraction of the CRDM flange structures (those near the central core location) were mocked up.

The test chamber was 1.8 x 2.5 x 2.5 m; it was formerly the sump beneath the SPERT-II reactor. The contents of the pit were designed to mock up the kinds of targets and reflecting surfaces that might be expected

within the cavity at TMI-2, at both near and far distances from the probe. Figure 16 shows the test chamber before filling with water. The pit contained loose arrays of standing "fuel" rods (mocked up by tubing), jackstrawed rods both standing and lying on the floor (more tubing), broken "fuel bundles" (compact arrays of tubing), and suspended rod fragments (which do not show in the figure). There were suspended flat surfaces in addition to the walls of the pit, mocking up fuel end boxes and core-formers, respectively. Crushed gravel on the floor of the pit and on the tops of the broken fuel bundles simulated the debris then known to lie at the bottom of the cavity at TMI-2. The gravel on the floor was arrayed in hills and valleys to partially simulate the suspected configuration at TMI-2.

This arrangement provided the first full-range testing of the system. Most details of system adjustment and operation were worked out in this geometry, and procedural details were refined.

The service-structure mockup provided the opportunity for training the personnel, and their backups, who would do the actual assembly at TMI-2. Details of the assembly procedure were worked out before containment entry by the assembly crew, down to the level of the exact locations on the service structure at which it was desired to stage the components. The final procedure amounted nearly to a complete choreography of the process; this was necessary to minimize personnel exposure to radiation and maximize the time available for operations. The final few assembly operations were performed in complete anticontamination clothing.

A deliberate effort was made to mock up the electrical noise characteristics that might be expected at TMI. This included a mockup of the existing length of TMI-2 cabling that would be used for digital communications between the console and the support structure in containment. (This wiring consisted of about a kilometer of #14 heavy-duty extension cord, nearly every bit available in Eastern Idaho.) This cabling was coiled and otherwise arranged to provide the maximum opportunity for inductive, radiative, and electrostatic noise pickup. SPERT-II is now a



Figure 16. Chamber for systems operations test. The sump below the former SPERT-II reactor is shown after installation of test targets and before filling with water. Fuel bundles and individual fuel rods on the floor and stacked in the corner of the pit are mocked up with small-diameter tubing and pipe. Crushed gravel on the floor and the tops of fuel bundles mock up known debris. The pit measured 2.44 x 2.44 x 1.8 m. (EG&G Idaho photo 83-6-2-9.)

machine-shop facility; its daily routine included use of machine tools, large motors, and arc welders. With some work, the system passed this noise test. The results did show, however, that the 10-MHz transducers would have marginal signal/noise ratio in this environment.

The data obtained during the systems operations tests were used to verify the intended analysis procedures. (These are detailed in the Results and Discussion section below.)

Personnel Training

Success of the TMI-2 data acquisition effort depended ultimately on the operating personnel selected for the project and development of the necessary skills through intensive training.

The operating crew consisted mainly of the principal designers of the equipment. These individuals, above all others, could be expected to know their product well from a standpoint of operating objectives, environmental limitations, design requirements and assumptions, hardware details, and the operational philosophy embodied in the specific combination of hardware and software. They also represented the most likely group with both knowledge and incentive to make the system work as required.

Both formal and informal operational training programs were conducted in parallel as part of the entire testing sequence. A deliberate effort was made to provide both cross-training and individual backup capabilities for all key functions. As stated earlier, the equipment being tested was used by the personnel being trained, to the benefit of both.

The final portion of the training effort took place at TMI-2. The nature of the environment mandated on-site radiation and containment entry training to meet TMI-2 worker safety requirements. In addition, the crew perfected their operating procedures using a detailed mockup of the TMI-2 reactor.

DATA ACQUISITION AT TMI-2

As described in the previous section of this report, certain preparatory operations were conducted at TMI before the actual core topography data acquisition began. These operations included (a) equipment checkout, (b) procedure rehearsals using the TMI mockup of the reactor upper support structure, and (c) final personnel rehearsals and training.

The in-reactor operations were conducted under more relaxed time constraints than had previously been expected, but were easily completed in the time originally allotted. Each operation is described below.

The initial containment entry, equipment setup, and testing were completed in 45 minutes, with less personnel exposure to radiation than had been estimated. Equipment testing included a rapid, but very thorough series of checks which verified that all functions of the system were, in fact, operating correctly before insertion of the probe into the reactor. The checks included quantitative measurements of the sensitivity of each transducer and its electronics. A reconnaissance survey followed, to define the main features and make scoping measurements within the core cavity and to allow optimum parameter settings for the detailed study. The reconnaissance survey consisted of three parts. The first was to verify the expected relationship between the initial probe location at its upper zero point and the structure of the lower plenum. This relationship is shown in Figure 17. The measurement was done with the 10 MHz, 90-degree (horizontally-pointed) transducer. It was concluded that the predicted locations were accurate to the approximately 8-mm resolution of the ultrasonic methods used to verify it.

The second part of the test was a careful survey of the recess in the upper grid plate in which the upper end of a fuel box formerly resided (Section G-G in Figure 17). Since this recess was oriented parallel to the cardinal directions of the reactor assembly (basically, plant north), this test provided a calibration of the orientation of the probe system.

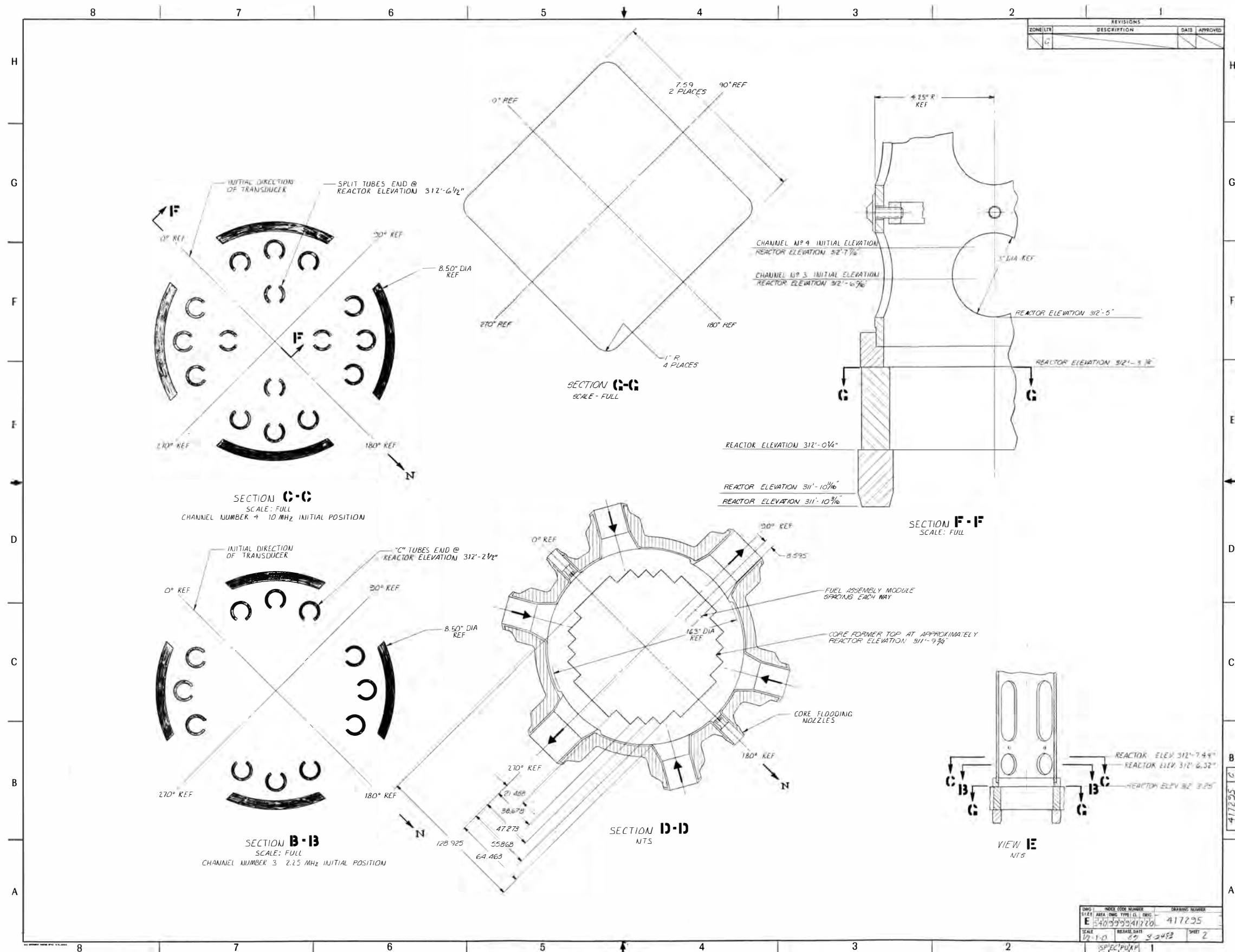


Figure 17. Structures in the lower plenum below, and potentially visible from, the uppermost probe position. NOTE: The initial measurements of the reconnaissance survey verified the dimensional relationships shown on this drawing for use as vertical benchmarks for the later full-cavity survey. The sides of the rectangular cavity shown in Section G-G served as the angular calibration of the system relative to plant north. The dimensions were verified as correct, within the dimensional resolution of the system.

Careful measurements showed that the probe system orientation had been rotated 6.43 degrees clockwise from the intended direction. The last part of the reconnaissance survey consisted of a survey of the cavity with vertical increments of roughly 250 mm. All transducers were tested during this survey.

There were difficulties. There was significantly more electrical noise on the 10-MHz channels than had been expected. There was enough noise to prevent their use at ranges much beyond 500 or 600 mm; there were no structures within the cavity this close. The unexpectedly large noise contribution is attributed to the ground arrangement within the existing TMI-2 cabling. The survey had to be made completely with the 2.25-MHz transducers. In spite of the full-system checkout before insertion in the reactor vessel, two of these transducers failed to produce usable output during the reconnaissance survey.

The reconnaissance survey established that the cavity was roughly cylindrical, with a depth between 1.5 and 2 m and a diameter of about 3 m.

The reconnaissance survey also established that the temperature of the water in the core was about 35°C, and that it was about 1°C warmer at the bottom of the cavity than at the top, with very slow convection. These were roughly the expected conditions for best operation of the system. Measurements made over two successive days showed stable temperature distributions, contrary to what had been expected.

A full-cavity survey was made with the three fully operative transducers. A model of the cavity was made by stacking electrostatic-transparency copies of the plots from the horizontal transducer between previously-prepared layers of transparent plastic. This model enabled visualization of the basic features of the cavity except for its floor and major portions of the top; it could be determined that there was a significant amount of material hanging from the upper grid plate, however.

A second survey was performed the following day, and it was found that the two 2.25-MHz transducers which had not worked the first day were fully operative. This complete survey was used in the final analysis. The reasons for the initial failures of the two channels are not fully understood, nor is the reason for their return to service; it is speculated that thermal expansion and/or vibration within the highly-compact remote pulser/receivers, causing short circuits, was probably to blame.

The in-containment systems were removed during an entry on a third day. Total man-hours in the containment building and cumulative radiation exposures to personnel were substantially below original estimates. These results reflect the positive effects of the team's commitment to ALARA policies throughout the project.

DATA REDUCTION AND ANALYSIS

Final processing of the data was done at the INEL. A three-step process, involving computerized sampling and redistribution, manual conditioning, and computer-aided drafting (CAD), yielded a matrix of contour maps of the core cavity. These maps could be correlated with video scans of the cavity and provided an adequate basis for constructing a physical model.

Data Sampling and Redistribution

The first processing setup was performed on a CDC-176 (Cyber) computer. Given the horizontal and vertical positions of the probe, its pointing directions, and its geometry, the three-dimensional locations of all ultrasonic reflectors were calculated. Approximately 5×10^5 individual measurements were processed. These locations were then plotted in both orthogonal and polar modes.

The orthogonal plots consisted of 51-mm thick slices in three mutually perpendicular directions. Each slice identifies the geometric locations of all reflectors ("hits") within that volume. A fourth plot orientation provided 2-degree volume sectors about the core vertical axis or centerline. Each plot extended from top to bottom of the cavity.

At this point there remained the problem of inaccurate values for the polar pointing angles of several of the transducers. These were redetermined from information contained within the data. At a number of locations the same reliably-identified reflective surface could be seen by two or more transducers, including the 90-degree (horizontally-pointing) transducer. These "calibration" targets were always chosen to be on vertical surfaces. It can be shown that, under these conditions, the actual pointing angle of the 90-degree transducer does not matter, that the returning echo always follows a path which is perpendicular to the target (i.e., the shortest path) and therefore is accurately horizontal, even though the major portion of the beam may not be exactly horizontal. Given

the apparent locations of the calibration targets and their errors relative to the 90-degree transducer, angular pointing errors were determined. The errors varied from 0.5 to about 2.0 degrees. The final plots were made with these corrected values.

Manual Conditioning

Manual operations on the data were artifact removal, view correlation, and contour checking. After computer processing, a variety of artifacts still remained in the data. Their removal was necessary in order to maximize the value of data and make its use easier. Only manual methods were effective, since the sorting process involved judgment calls:

- For threshold comparisons, identify and eliminate noise.
- For multiple bounce ghosts, identify the geometry which caused them and eliminate them.
- Where corner traps are indicated, are they ridge or valley?

View Correlation

One difficulty was encountered during view correlation among the four plotting orientations. At long distances from the probe, the "hits" tended to be sparse, as a result of large range and unfavorable reflector orientation. (Ideally, the surface of interest should be as nearly as possible perpendicular to the slice being examined.) The actual correlation process involved transfer of locations to the appropriate horizontal planes. For adequate coverage it was often necessary to interpolate between blank areas from known data. Coverage of some shadowed areas was achieved by interpolation or extrapolation, as required.

Contour Checks

Within a given horizontal presentation, two checks were always performed. First, the contour must be continuous. Second, the contour

must be credible in the context of adjacent slices. All contours were traced and checked to ensure that these requirements were met and cross-compared with original slice plots.

Computer-Aided Drafting

The objective of the CAD operation was to produce a series of final contour maps which, in combination, would provide the needed information for damage evaluation and core recovery efforts. Manually conditioned contour data were input to the CAD system via a tablet-entry facility track ball. Individual contours were then scaled and correlated. Finally the results were summed and plotted in three groups. The least confusing of the groups was selected for the final maps, and finishing notations were added by hand. The maps are shown as Figures A-1 through A-5 in Appendix A. The original maps were made in 3/16 scale.

Model Building

A subsequent effort translated the data from the individual contours into a three-dimensional scale model of transparent acrylic resin (Lucite), each layer of acrylic corresponding to one 51-mm contour interval. In this manner the data were integrated to provide visual convenience and a readily portable display.

Error Analysis

Contributions from 13 different error sources were evaluated as part of the overall analysis. The largest magnitudes were associated with line positioning and width, system calibration and related temperature effects, and the range data digitization process.

The errors of measurement were analyzed for a range equal to that of the nominal position of the core-former walls (1.62 m) and expressed in linear dimensions at that range. The systematic and random errors were estimated separately on a conservative basis, then adjusted individually to reflect an overall conservative uncertainty in the random component.

The random errors which contributed to the uncertainty in the measured speed of sound included those in the base data (literature values) on which the calibration was based, the precision of the replicated speed of sound measurements made during operations at TMI-2, and errors attributable to the fact that the water in the cavity was not isothermal. The measured vertical temperature gradient was about 0.6°C , as inferred from the speed of sound. A linear horizontal gradient of 1.2°C from the probe to the walls was assumed. The effects of these gradients were folded into a term which is designated as errors in range measurement due to convection. Refractive errors in beam plotting angle due to these gradients were shown to be negligible.

Errors due to mechanical sources included eccentricity and vibration of the probe and boom. Eccentricity errors were caused by the fact that the boom was not perfectly straight; these were estimated from detailed measurements made on the recess in the upper grid plate and represent the uncertainty which is left after removal of the systematic error attributable to imperfect centering of the mechanism on the CRDM flange. Vibration amplitude was estimated from large-scale plots of data from single transducers at single elevations.

The range-measurement digitization interval leaves an uncertainty of plus or minus one digitizing interval on the location of the surface measured.

Errors potentially arising from the slice-plotting process included those due to the finite spacing of the nibs on the (dot) plotter used and to the stability of the paper on which the plots were made. This latter was estimated from repeated plots, after removing the nib-spacing uncertainty.

The manual steps introduced errors which were more difficult to estimate. The width of pencil lines was measured on full-reactor-size blowups of typical manual plots. The reproducibility of the position of these was estimated in a similar manner, using areas which had been

replotted (without reference to estimation of errors) for various reasons. Similar estimates were made for the manual tablet-entry step.

The known systematic errors were removed by an appropriate change of scale on the final plots. The random errors, which reflect the overall uncertainty of range measurements at the approximate range of the core-former walls, are summarized in Table 2. The final overall error estimate is taken as the square root of the sum of the squares of the individual error components. This value is 13.1 mm.

The range uncertainty at the core-former walls was ± 13.1 mm. At the upper grid plate, the range accuracy was ± 18 mm, and at the floor it was about 40 mm. Lateral resolution was approximately 40 mm in all locations.

TABLE 2. COMPONENTS OF RANDOM ERROR

<u>Components</u>	<u>Magnitude^a (mm)</u>
Calibration base data	±4.1
Operational calibrations	±2.7
Convection	±2.0
Vibration and eccentricity	±5.3
Range digitization	±3.8
Plotter resolution	±2.0
Paper stability	±0.6
Line width	±3.8
Line position reproducibility	±7.6
Tablet entry	±4.0
Final CAD plot	±3.0

a. At core-former wall

RESULTS AND DISCUSSION

An appraisal of the TMI-2 core topography data acquisition project should be made from two different viewpoints: (a) the direct significance and value of the techniques used and the physical knowledge obtained and (b) the broad implications of a very versatile computer-controlled remote measurement technique useful in remote and hostile environments.

The primary output of the CTDA system was a series of drawings of individual contours. The contours were processed into four topographic maps of the core cavity. For mapping, the cavity was divided into three regions, according to probe position measured from the bottom of the upper grid plate:

- Bottom, from -198.1 to -106.7 cm (-78 to -42 in.)
- Central, from -101.6 to -40.6 cm (-40 to -16 in.)
- Top head, from -35.6 to -5.1 cm (-14 to -2 in.).

The fourth map is an upward-looking view (mirror image) of the top head, to complete the internal coverage. These drawings are included in Appendix A of this report.

Further aids for visualizing the TMI-2 core topography have been constructed from the data. These aids include perspective views, ultrasonic images, and a three-dimensional Lucite model.

The perspective views are based on octants of the cavity volume. They were intended to provide a detailed physical image of the core state by volume sections rather than slices.

The original data were used to produce a series of ultrasonic gray-scale images of the interior of the cavity in a separate computer operation. The images were produced by assuming a viewpoint along the

centerline of the probe and projecting the location of each "hit" onto picture elements (pixels) in a flat plane representing a 360-degree panorama around the viewpoint. The range to each pixel was encoded in the image along a gray scale that placed white near the probe and black at maximum range. One such image is shown in Figure 18. In this case, the viewpoint is perpendicular to the centerline of the probe. Note that, since this was entirely a computer operation, the image contains both noise and ghost artifacts, which result in a somewhat more smeared image than was eventually obtained in the final maps. These images were in fact the first visualization of the entire cavity; they were used to orient data-reduction and project personnel during data analysis. They were also used as references to resolve structures and configurations that might otherwise have been ambiguous.

The most striking visual aid is the three-dimensional Lucite model of the core cavity, shown in Figures 19 through 21. This model is based on the calculated three-dimensional positions of all distinguishable sound-reflecting surfaces within the cavity. Part of its value is that it physically depicts the entire cavity. It thus provides perspective and context for both contour data interpretation and operation planning. It is also a direct check on the results of video scans.

Data Summary

The ultrasonic measurements describe a cavity of 9.3 m^3 , about 26% of the total volume of the core region. The average depth of the cavity is about 1.5 m, with the lowest measured location being nearly 2 m below the upper grid plate. Considerable debris hang from the upper grid. The radial extent of the cavity approaches full core radius, with core-former walls exposed in places. Sections of fuel rods, some of them broken and overhanging, line portions of the sides of the cavity. The floor of the cavity consists of a series of debris-covered ridges and valleys with jumbled fuel rod sections in some locations.

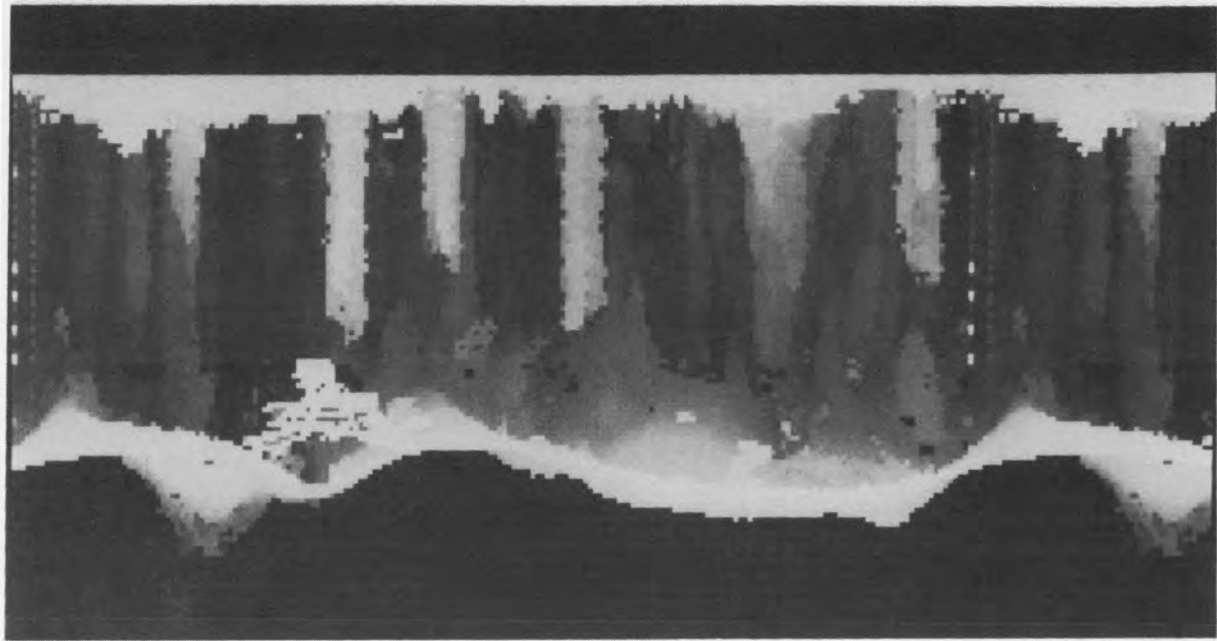


Figure 18. An ultrasonic computer image of the core cavity in TMI-2. The image is a 360-degree panorama with a viewpoint perpendicular to the centerline of the core. The range from the centerline is coded in shades of gray; targets close to the probe are bright, while those farther away become darker with range. The floor of the cavity has several deep valleys. Debris are piled near the core-former walls in places. Five of the objects hanging from the roof in the middle distance are axial power shaping rods; the sixth (second from right) is a series of broken fuel rods also seen in Figure 22. Considerable debris hang from the ceiling. The bright object near the 120-degree point is a fuel end box.

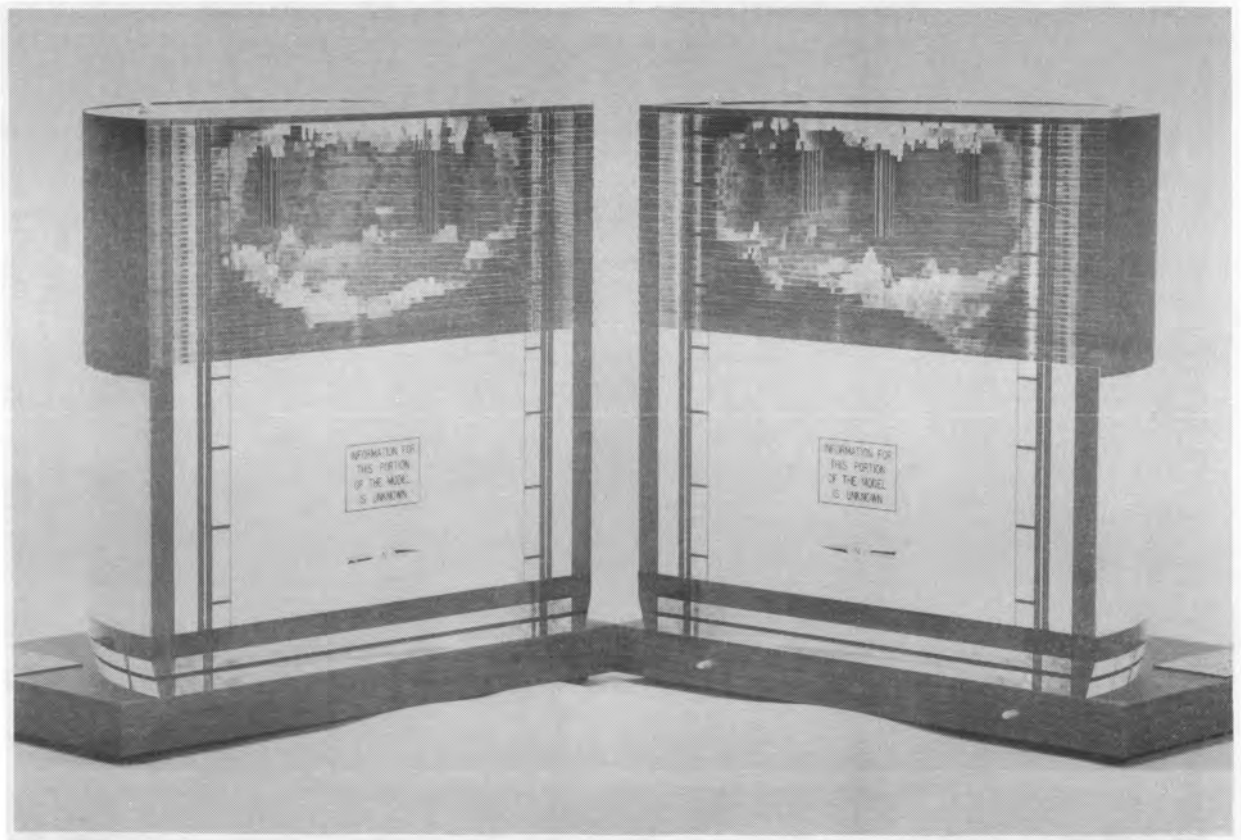


Figure 19. Plastic model built to 3/32 scale, showing the cavity in relation to the full core. The model is built in halves. The individual layers in the cavity region represent 51 mm (2 in.) of contour elevation. They correspond to the contours shown in Figures A-1 through A-4 in Appendix A. (GPU Nuclear Corporation photo.)

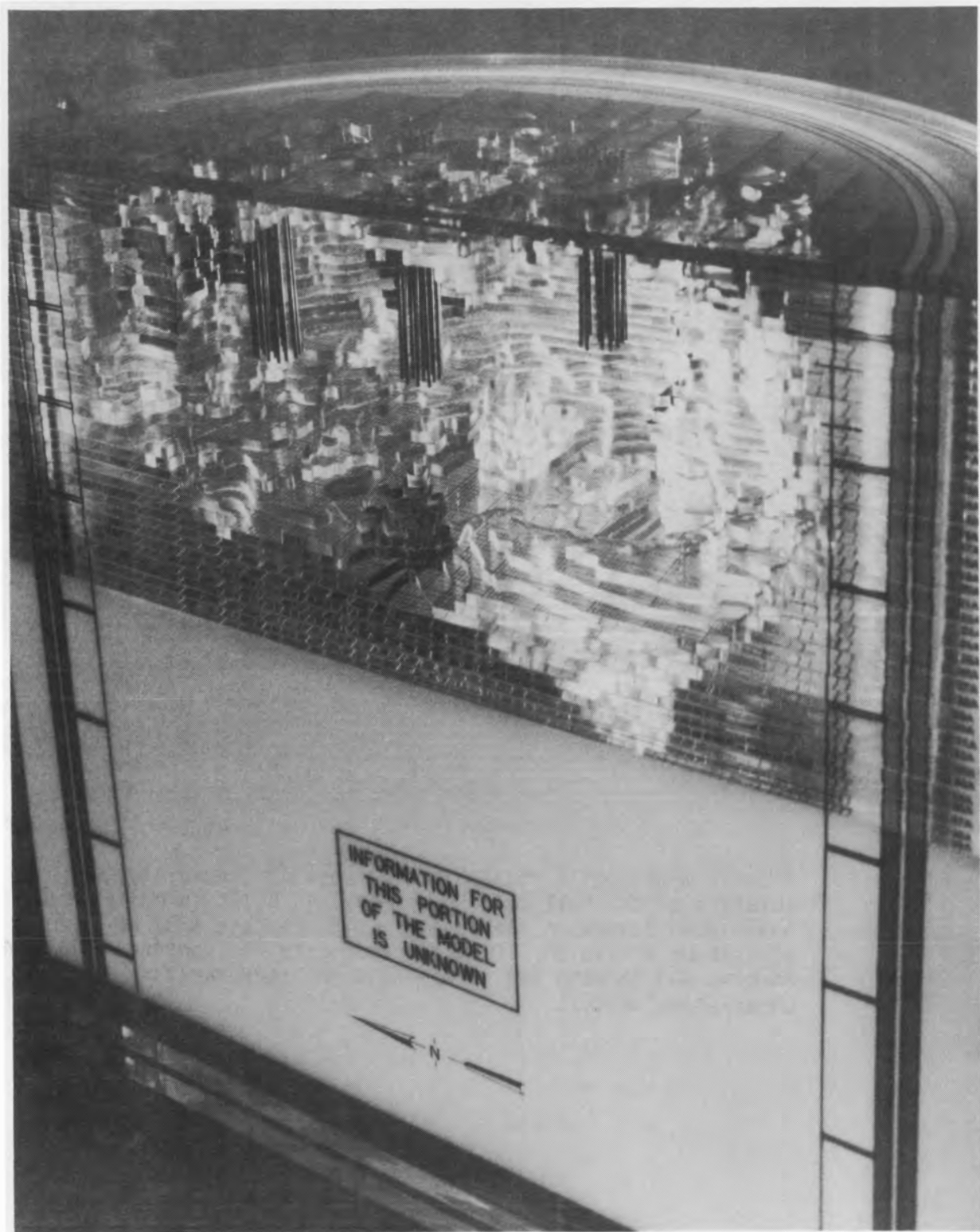


Figure 20. View of half of the plastic model. This corresponds to the first 180 degrees of the panorama shown in Figure 18. (EG&G Idaho photo 83-632-1-9.)

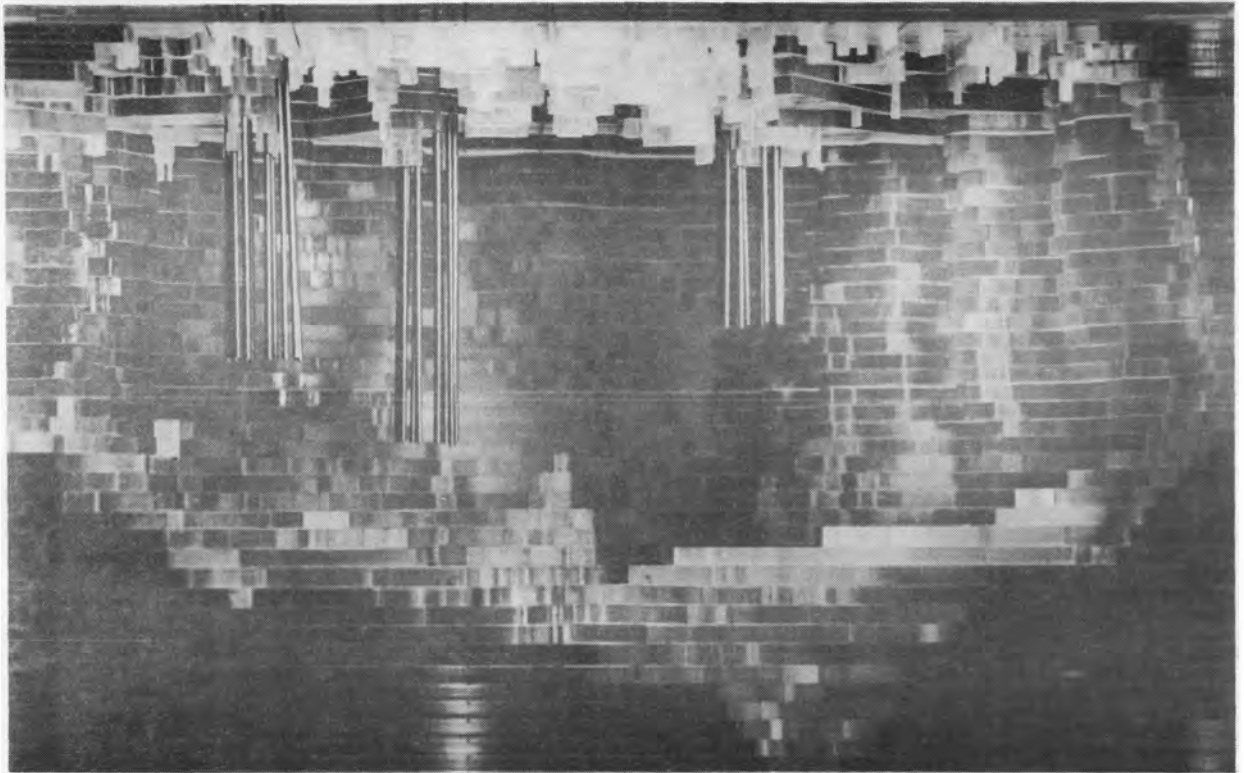


Figure 21. Closeup photograph of the plastic model, showing the first 180 degrees of the data shown in Figure 18. The individual layers of the model represent 51-mm (2-in.) contours within the cavity. The rods represent the locations and approximate lengths of the axial power shaping rods within the core at the time of measurement. (GPU Nuclear Corporation photo.)

No more than 42 of the core's 177 fuel assemblies have any full-length fuel rods remaining in the region of the cavity. Only two fuel assemblies (at locations A-6 and C-3) appear to be totally intact through this region, and four more appear to be largely (>95%) intact. The remaining fuel assemblies defining the vertical wall of the cavity have portions missing from the top five feet (1.5 m), ranging from roughly 5% to 90% of their cross sections.

Five of the axial power shaping rods (APSRs) protruded partially into the cavity at roughly half core radius during these measurements. These can be seen in the middle distance (medium gray tones) in Figure 18, and simulated in photographs of the model (Figures 19 through 21) by short rods. The ultrasonic data show that these APSRs are distorted and have irregular lower ends. The APSRs shadowed a large portion of both sidewall and cavity ceiling; data have been interpolated and extrapolated in the shadow areas.

Much material is suspended from the upper grid plate. The bulk of it is less than 0.3 m in length. The material is highly irregular in length and shape, though there is a tendency for the suspended material to be aligned along the edges of former fuel assembly locations. The suspended material is visible in Figures 18 through 21 and in Appendix A, Figures A-1 and A-2. The complex and irregular pattern of the suspended debris combined with the APSRs to give a gradually increasing shadowed area as the radius increases. As a result, details of the suspended material in the ultrasonic results become sparser as radius increases, and the outer edges of the upper grid plate are almost totally obscured (Appendix A, Figures 1 and 2). From the ultrasonic data there does not appear to be a systematic change in the amount or kind of suspended material between the center and the outer edges of the upper grid plate, however.

The middle elevations of the cavity, from -16 in. through -40 in., are roughly cylindrical, the boundaries of the cavity generally following or passing through the outer ring of fuel assemblies with little regard to the actual fuel assembly locations, as seen in Figure A-3 of Appendix A. The

largest exception occurs along the southwest side of the reactor, where there appears to be more standing fuel than in most other locations. In the west-southwest direction there is an overhanging "peninsula" that can be traced from about -50 in. to the upper grid plate at zero elevation; it can be seen on Figures A-1 through A-4 of Appendix A, and as the second middle-distance object from the right in Figure 18. A still frame from a recent videotape (Figure 22) indicates that this structure consists at least in part of loose and broken fuel rods suspended from the ceiling.

Similar overhanging of the side walls of the cavity, though smaller in magnitude, is general through all parts of the cavity. This can be inferred from the maps of Figures A-1 through A-4 in Appendix A, and more dramatically in Figure A-5 of Appendix A.

The core-former walls are exposed in a number of places. The largest exposures are on the east side of the core at locations P-5, R-6, and R-7, as seen in Figure A-3 of Appendix A. The ultrasonic measurements of range show the core-former wall in parts of these areas to be deformed outward as much as 70 mm; the outward deformation can be traced from elevation -14 in. to about elevation -42 in. A very thorough error analysis, combined with auxiliary tests of data consistency, lend credence to the reality of the measured deformation; note that the conservative estimate of range errors at this location yields an uncertainty of less than 14 mm.

The floor of the cavity is mapped in Figure A-4 of Appendix A. The three low spots in the cavity floor are near locations B-10, F-5, and P-5, respectively; the lowest measured elevation is slightly more than -78 in. at P-5. The configuration of the debris bed in the vicinity of these low spots suggests that these locations were flow channels. The low spot at P-5 is heavily overhung (Figure A-4 of Appendix A). It can be seen in the foreground in Figure 20 and to the right side of Figure 18.

Fuel assembly end-fitting and spider combinations appear to have fallen onto the debris bed at a number of locations as a result of disconnection of CRDM lead screws before the initial video surveys. The

most prominent of these is centered near location K-8. It can be seen in the left foreground in Figure 18, near the center of Figure 20, and in Figure A-4 of Appendix A. It is also shown in cross section in Section B-B of Figure A-5 of Appendix A. Another such combination can be seen at location O-8 in Figure A-4 of Appendix A. Others can be inferred in Figure 18.

Previous videotape surveys did not provide a detailed or accurate description of the core cavity. A more recent and more extensive video scan was interpreted with the aid of the ultrasonic results. Its content confirms and supplements the ultrasonic data.

Figure 22 comes from that videotape. It shows a portion of the structure mapped in the west-southwest direction in Figure A-3 of Appendix A and discussed above; it confirms the ultrasonic interpretation of this structure as a loose and irregular surface, inferred from severe "ghosting." Figure 23 is a videotape frame showing the debris bed nearly below the probe. The debris bed in this area consists of rubble with a few larger pieces of unidentified material and two fuel-rod springs.

Figure 24 shows another area of the cavity floor where broken fuel rods are strewn like "pickup sticks." These individual rods had not been imaged well ultrasonically; they appeared ultrasonically as scattered bright spots where specular reflectivity toward the probe was highest, but without any indication of their shape or of the surface on which they rested. They were therefore omitted from the maps. They can be seen as scattered bright spots in the right quarter of Figure 18.

Project Overview

A survey of the completed project and its broad implications shows that positive aspects prevailed.

1. An interdisciplinary team successfully carried out a disciplined design effort, procurement from suppliers, fabrication, testing,

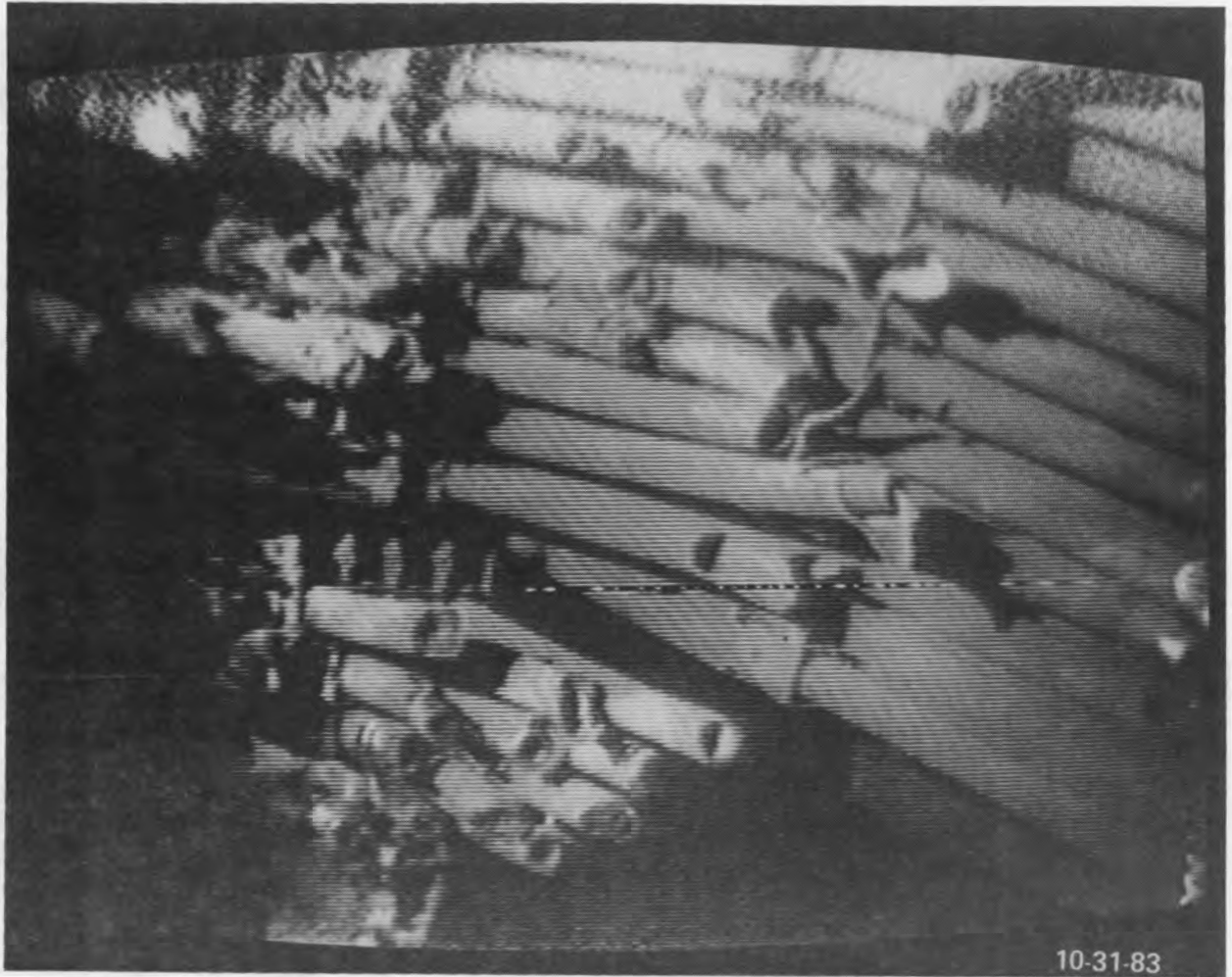


Figure 22. Structures in the west-southwest direction on ultrasonic maps. Looking upward, the video camera photographed stub ends of broken fuel assemblies that are adhering to the bottom of the reactor's upper plenum structure. Fuel rods are 11 mm (0.43 in.) in diameter. (GPU Nuclear Corporation photo.)

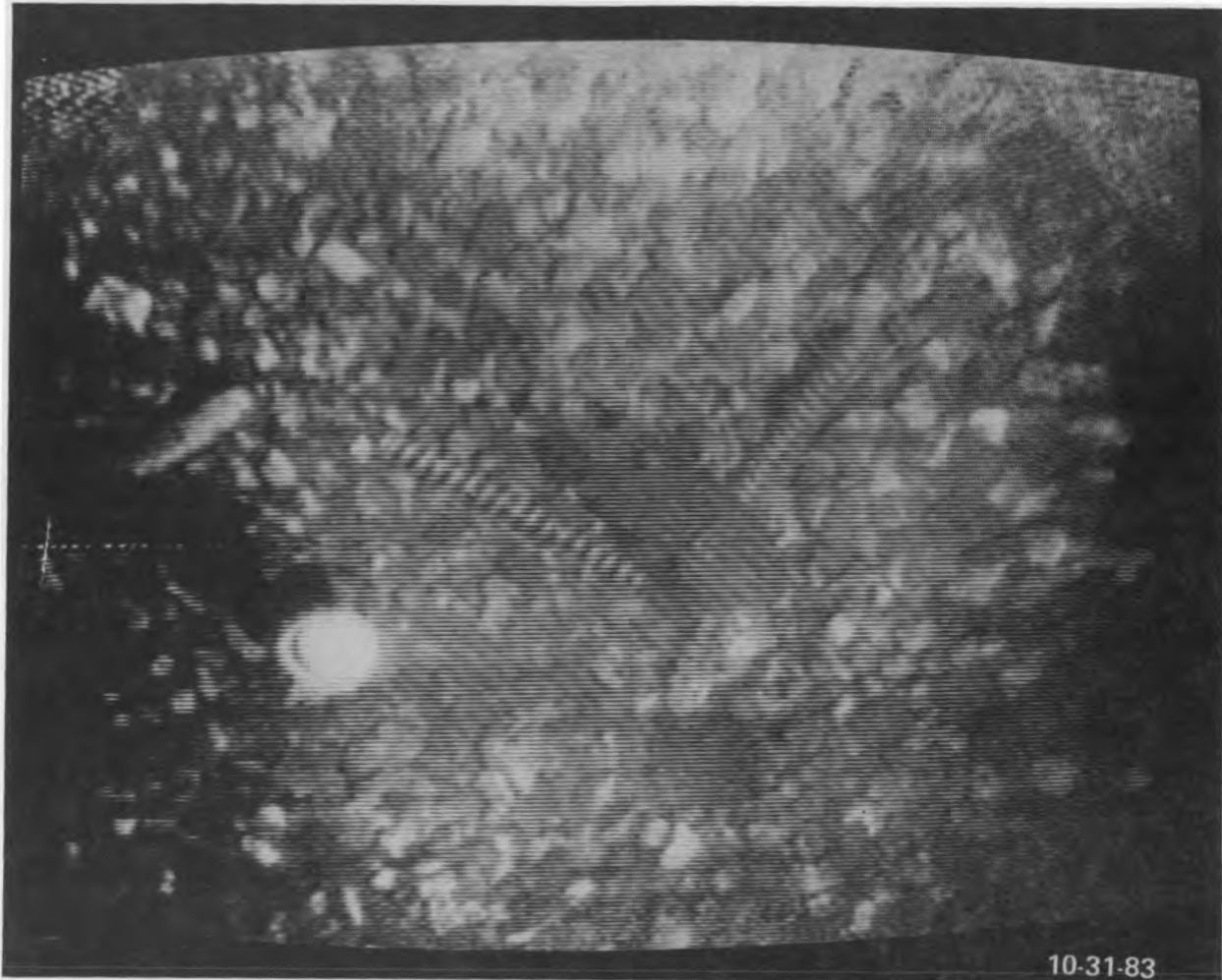


Figure 23. Rubble bed beneath the probe location. Looking down, the video camera photographed the surface of the rubble bed, showing fuel rod springs and pieces of rubble. (GPU Nuclear Corporation photo.)

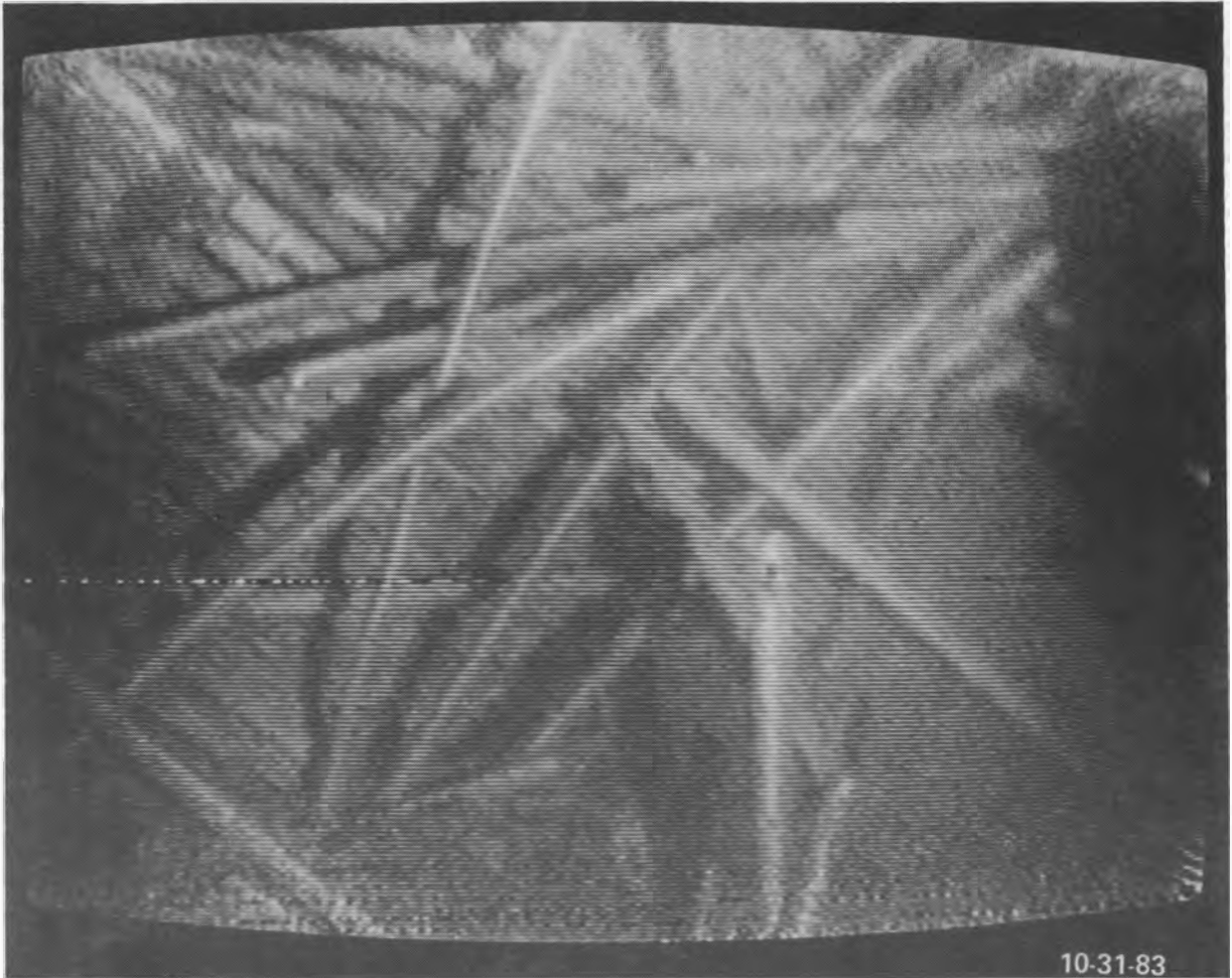


Figure 24. Broken fuel rods on the floor of the cavity. Loose and broken fuel rods lie on the floor of the cavity in one of the valleys. These were imaged poorly by ultrasound because of the specular and highly-directional nature of sonic reflections from their randomly-oriented surfaces. (GPU Nuclear Corporation photo.)

and personnel training within 4-1/2 months, certainly less than the already tight 5-month time allotment. A combination of wide expertise, careful attention to assumptions, and outstanding cooperation helped make this achievement possible.

2. No major mistakes were made in either assumptions or operations. All major items were anticipated and handled reasonably.
3. Few problems arose that were not expected. One example is the insufficient power from the 10-MHz transducers. Even here, a backup position (the duplicate, 2.25-MHz array) had been established.
4. The information obtained has at least a twofold value. First, it provides a firm basis for designing recovery procedures for the TMI-2 reactor. Second, it furnishes key information in reconstructing a detailed accident sequence and consequence.
5. Proven equipment and techniques from different technologies are uniquely combined for this application. Conventional ultrasonic nondestructive evaluation is restricted to much smaller distances, while conventional sonar ranging involves much larger distances; this system successfully bridged the two disciplines.
6. Subsequent applications are expected on the basis of inquiries received. The technology now available comprises a proven system and technique which was fully successful on first use.
7. The advantages of computerized data acquisition and control for detailed scanning and extensive coverage are well demonstrated.
8. The team commitment to ALARA policies throughout the project, in spite of the very short schedule, made a substantial and noteworthy contribution to the overall success of the project.

APPENDIX A

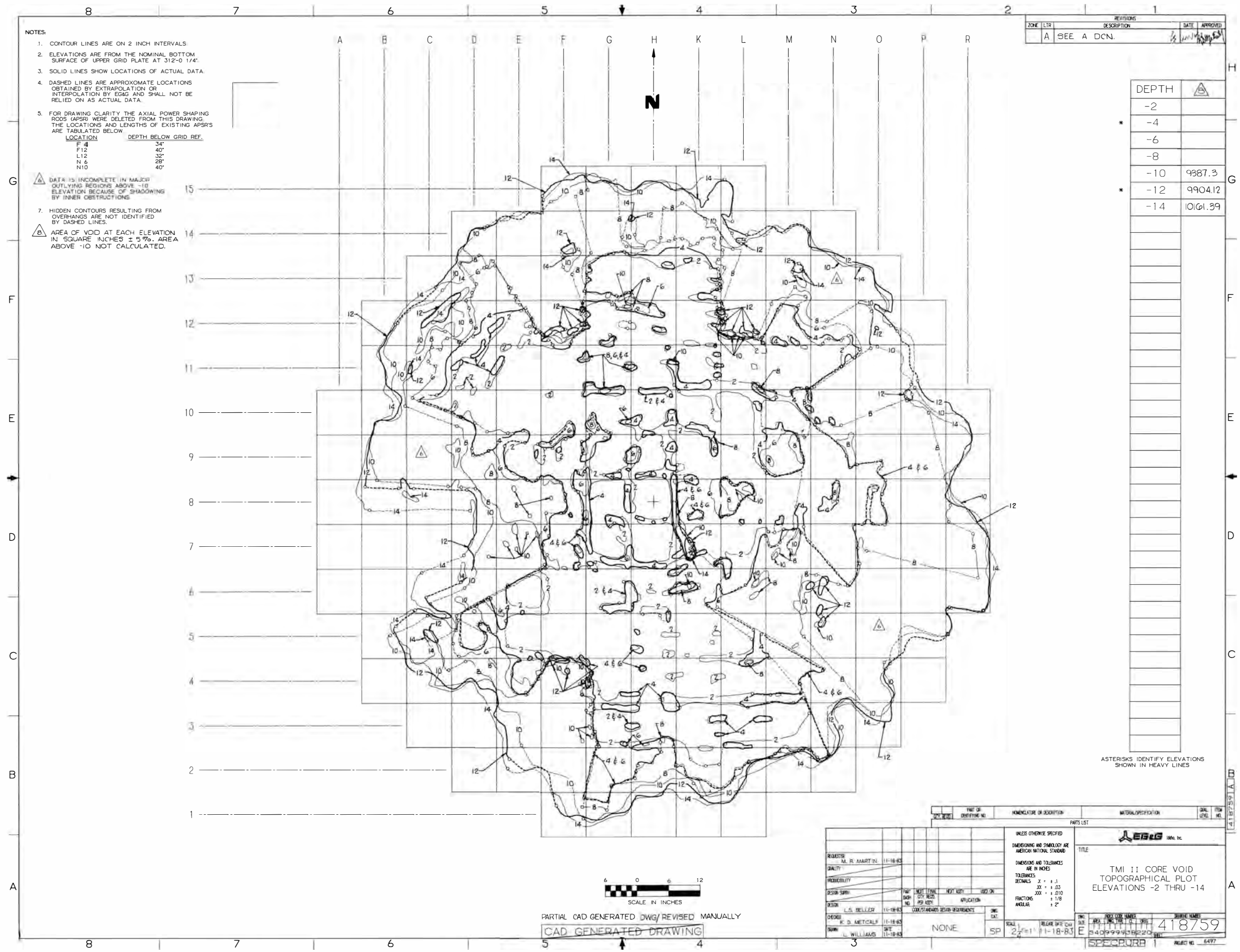


Figure A-1. TMI-2 core void topographical plot elevations -2 through -14.

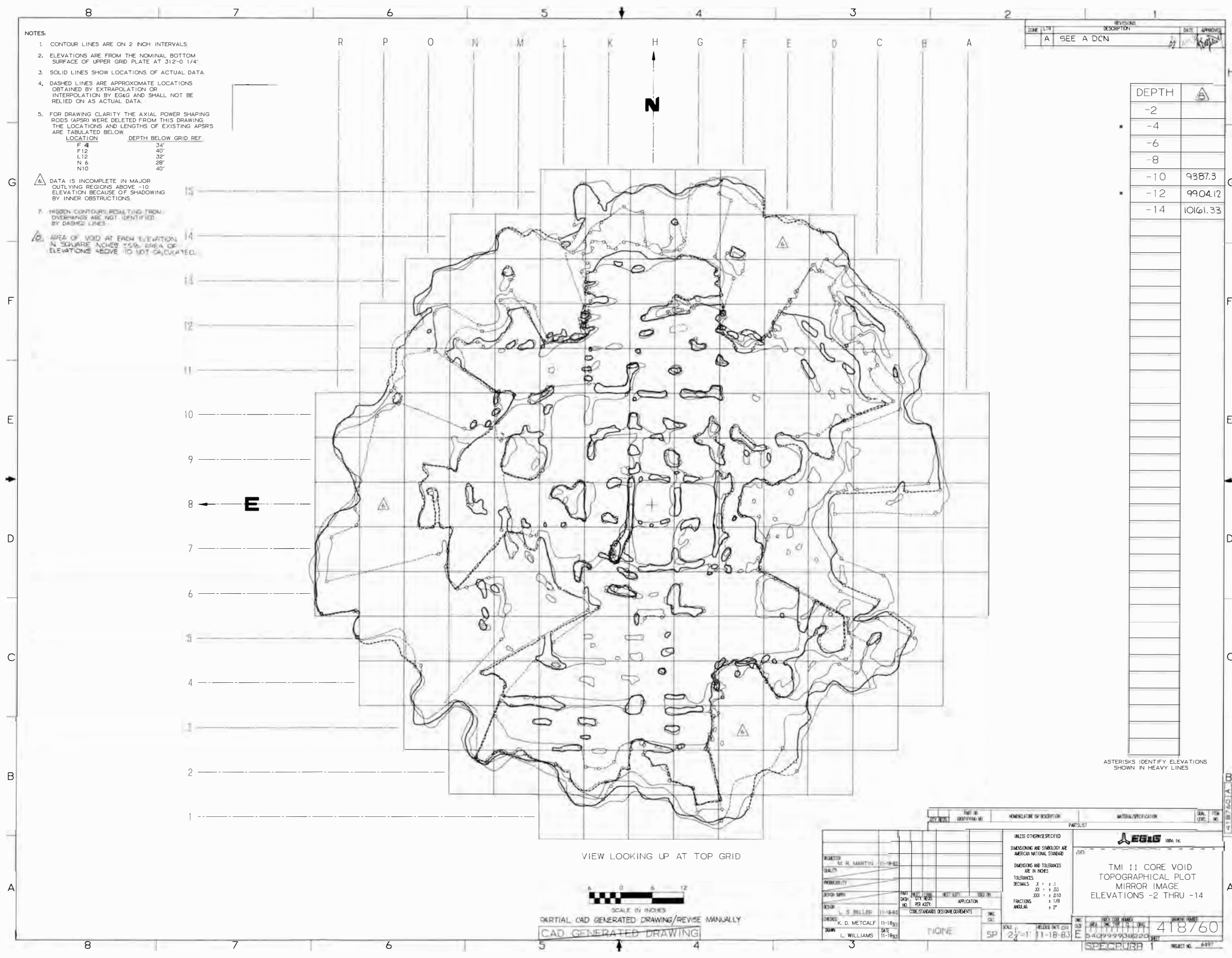


Figure A-2. TMI-2 core void topographical plot mirror image elevations -2 through -14.

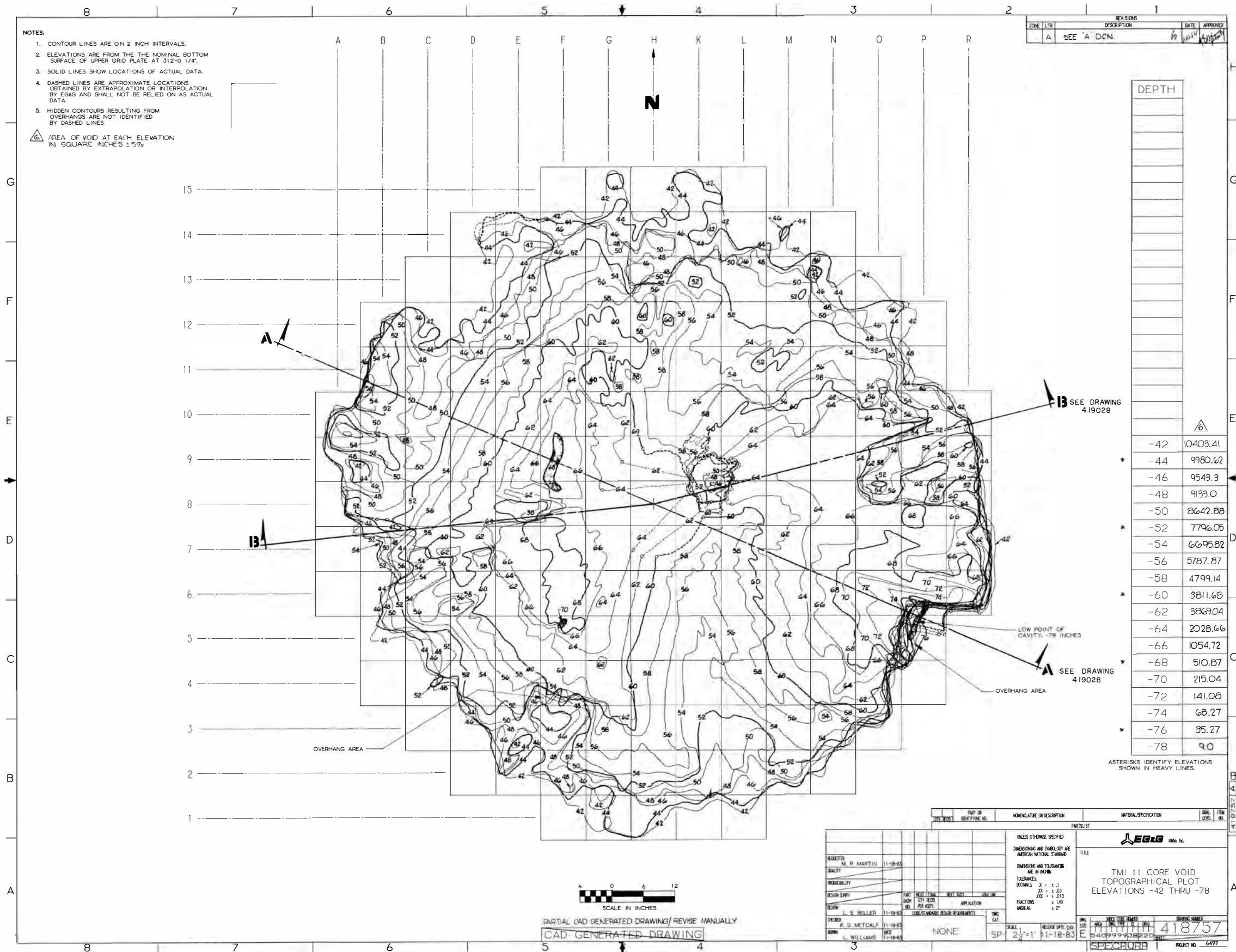


Figure A-4. TMI-2 core void topographical plot elevations -42 through -78.

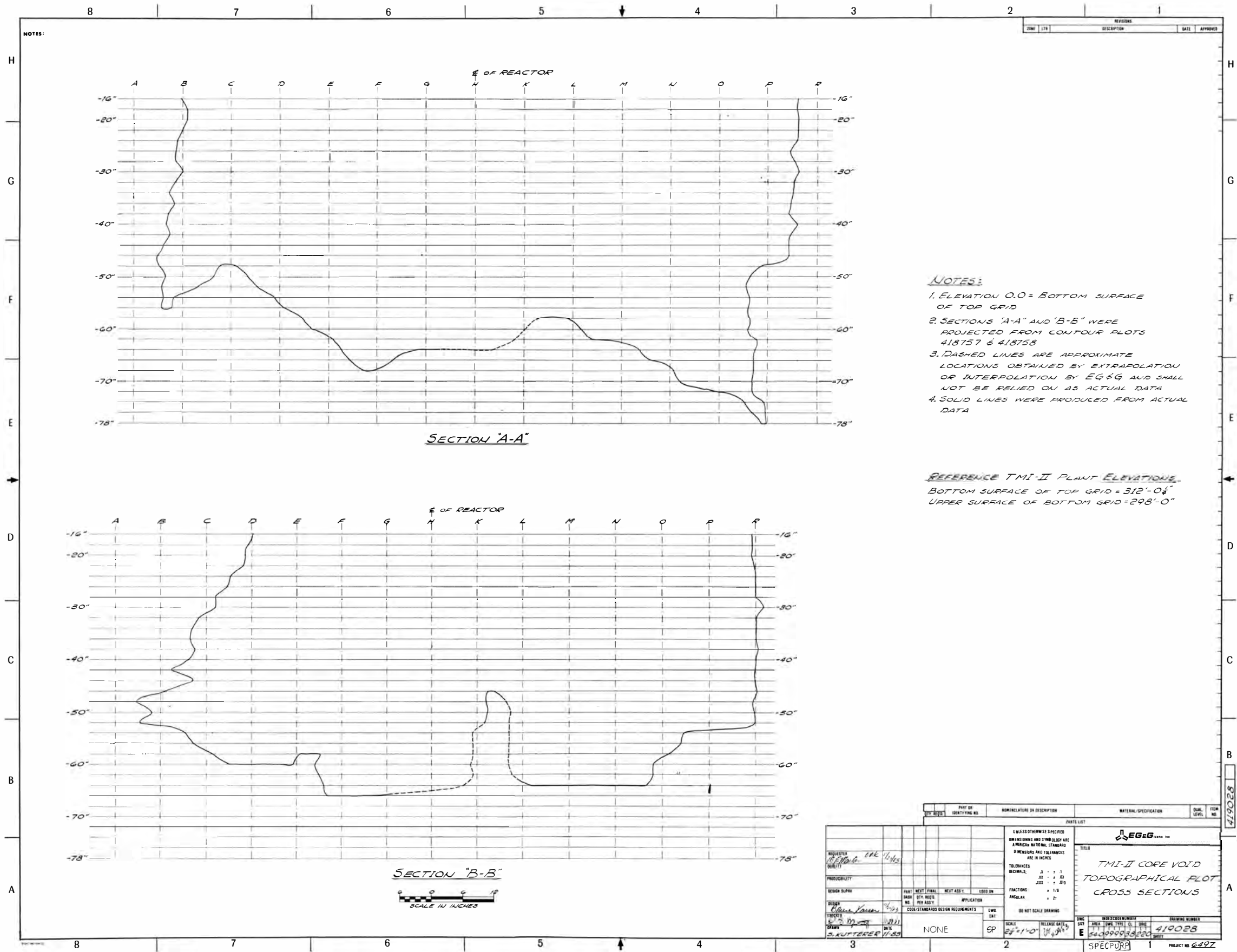


Figure A-5. TMI-2 core void topographical plot cross sections.

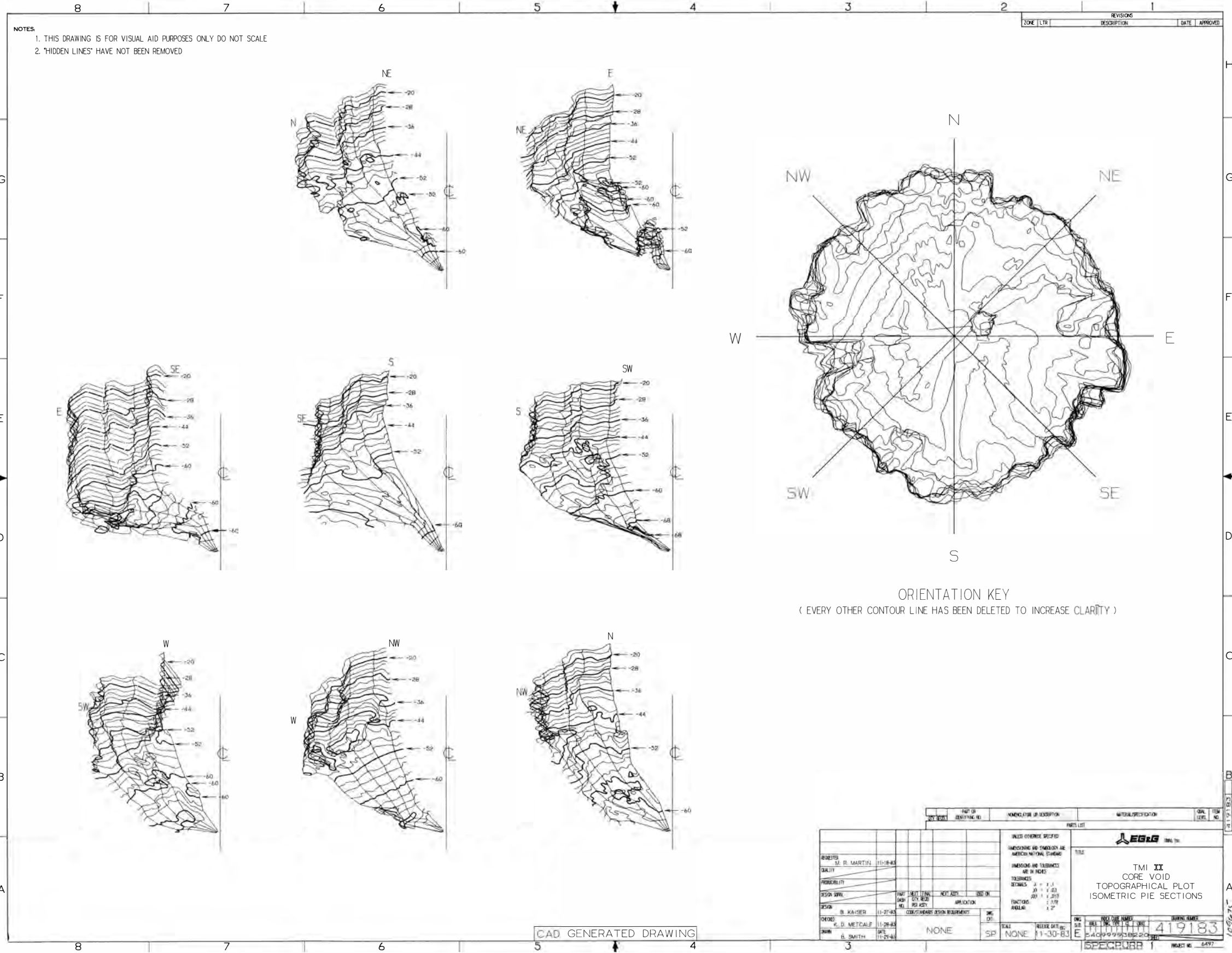


Figure A-6. TMI-2 core void topographical plot isometric pie sections.



A000022299185

Deacidified using the Bookkeeper process.
Neutralizing agent: Magnesium Oxide
Treatment Date: Feb. 2007

PreservationTechnologies
A WORLD LEADER IN PAPER PRESERVATION

111 Thomson Park Drive
Cranberry Township, PA 16068
(724) 779-2111



A000022299185